

Decision Making under Uncertainties for Air Traffic Flow Management

Guodong Zhu

Abstract

As a new strategic Traffic Management Initiative (TMI) in the FAA's NextGen portfolio, the Collaborative Trajectory Options Programs (CTOP) can manage multiple constrained regions in an integrated way with a single program and allows flight operators to submit a set of desired reroute options, which provides great efficiency and flexibility.

One of the major research questions in TMI optimization is how to determine the planned acceptance rates for airports or congested airspace regions to minimize system-wide costs. There are two types of uncertainties that need to be considered in setting CTOP rates: first, uncertain airspace capacities, which result from imperfect weather forecast; second, uncertain demand, which results from flights being geographically redistributed after their reroute options are processed.

In this paper, three families of stochastic models are proposed. The first family of models can optimally plan ground and air delay for groups of flights if the route choice of each flight is known. The second family of models control each individual flight and can give the theoretical lower bounds for the very general reroute, ground-, and air-holding problem. The third family of models directly control the queue size at each congested region, and can be solved more efficiently compared with the second family of models. Although these models can provide important benchmarks and can be used in an airline internal CTOP, they are not compatible with Collaborative Decision Making (CDM) CTOP software implementation. The simulation-based optimization model, which can use stochastic models as part of its heuristic, is proposed and can give good suboptimal solution to the practical CTOP rate planning problem.

This paper gives the first algorithm that optimizes the CTOP rate under demand and capacity uncertainties and is compatible with the CDM CTOP framework, and provides much-needed decision support capabilities for effective application of CTOP.

Nomenclature

Sets and Indices

\mathcal{C}	Set of ordered pairs of PCAs. $(k, k') \in \mathcal{C}$ iff k is connected to k' in the directed graph of PCAs
Ω_{ij}	Ordered set of indices of the airport/PCAs which flight i passes if taking route j
\mathcal{R}	Set of resources, including departure airports and PCAs
T_{ij}^r	Set of allowed time periods for flight i taking route j to depart from/pass through airport/PCA r
Φ_k	Set of indices of the routes which cross PCA k
Ω_{ij}	Ordered set of indices of the airport/PCAs which flight i passes if taking route j

Input Parameters

$\Delta^{k,k'}$	Number of time periods to travel from PCA k to k' , defined for all pairs $(k, k') \in \mathcal{C}$
p_q	Probability that scenario q occurs
$M_{t,q}^k$	Real capacity of PCA k in time period t under scenario q
t_s	Time period in which stage s begins
$S_{s,t,\rho}^k$	Number of flights with the same path ρ originally scheduled to depart in stage s and arrive in PCA k (direct demand) in time period t
N_b	Number of scenarios corresponding to branch b
o_b, μ_b	Start and end nodes of branch b
\underline{T}_{ij}^r	First time period in the set T_{ij}^r
\overline{T}_{ij}^r	Last time period in the set T_{ij}^r
N_{ij}	Number of PCAs along route j of flight i
t_{ij}^r	Time period in which flight i taking route j is scheduled to cross PCA r
Ω_{ij}^k	The k -th resource along route j of flight i
Dep_i	Original scheduled departure time of flight i
c_{ij}, c_g, c_a	Cost for flight i taking route j , cost for unit ground delay and air delay
ρ_1, ρ_{-1}	First and last PCA on path ρ

Primary Decision Variables

$P_{t,\rho}^k$	Planned direct demand at PCA k in time period t from flights with the same path ρ
$X_{s,t,t',\rho}^{k,q}$	Number of flights with the same path ρ , originally scheduled to depart in stage s arrive in PCA k (direct demand) in time period t , rescheduled to arrive in t' under scenario q

$P_{t,l,\rho}^{k,q}$	Number of flights with the same path ρ , flight time l (to the first PCA k on path ρ) and departure time t under scenario q
w_{ijt}^r	Whether flight i taking route j departs from/passes through airport/PCA r by time t
w_{ijt}^{rq}	Whether flight i taking route j departs from/passes through airport/PCA r by time t under scenario q
\tilde{w}_{ijt}^{rq}	Whether flight i taking route j reaches the first PCA r on route j by time t under scenario q

Auxiliary Variables

$P_{t,\rho}^{k,q}$	Planned direct demand at PCA k in time period t from flights with the same path ρ under scenario q
$D_{t,\rho}^k$	Scheduled direct demand at PCA k (from airports) in time period t from flights with the same path ρ
$G_{t,\rho}^k$	Number of flights with the same path ρ whose arrival time at PCA k is adjusted from time period t to $t + 1$ or later using ground delay at their point of origin
$L_{t,\rho}^{k,q}$	Number of flights with the same path ρ that actually cross PCA k in time period t under scenario q
$A_{t,\rho}^{k,q}$	Number of flights with the same path ρ taking air delay before PCA k in time period t under scenario q
$\text{UpPCA}_{t,\rho}^{k,q}$	Number of flights in path ρ arriving at PCA k in time period t from the upstream PCA in the same path under scenario q
$D_{t,l,\rho}^k$	Number of flights with the same path ρ , flight time l (to the first PCA k on path ρ) and with original scheduled departure time t
$G_{t,l,\rho}^{k,q}$	Number of flights with the same path ρ , flight time l (to the first PCA k on path ρ) receiving ground delay in time period t under scenario q
δ_{ij}	Binary indicator whether flight i will take route j
$\delta_{qti j}$	Binary indicator whether flight i will depart in time period t and take route j under scenario q
$\tilde{\delta}_{qij}$	Binary indicator whether flight i will take route j under scenario q

Acronyms and Abbreviations

AFP	Airspace Flow Program
ATC	Air Traffic Control
ATM	Air Traffic Management
CDM	Collaborative Decision Making
CTOP	Collaborative Trajectory Option Program
FAA	Federal Aviation Administration
FCA	Flow Constrained Area
GDP	Ground Delay Program

PCA	Potentially Constrained Area
RBS	Ration by Schedule
RTC	Relative Trajectory Cost
TMI	Traffic Management Initiative
TOS	Trajectory Options Set

1 Overview

1.1 Introduction

Air traffic flow management refers to strategic decisions made by air traffic managers to balance demand with capacity at airports and airspace regions, which includes modify flight departure time and trajectory. It is strategic in the sense these actions are applied proactively, hours in advance and usually affect a large region in the National Airspace System (NAS).

Air traffic flow management plays an essential role in ensuring safe and efficient use of national airspace. In the peak operational times, there are almost 5,400 aircraft flying at the same time in the national airspace. If there are some adverse weather conditions which cause capacity reductions in en route airspace and airports, or there are demand surges or accidents like closed runway, we will have the capacity and demand imbalance. If we cannot resolve these system disruptions properly, serious flight delays and cancellations will happen, which can have significant economic impacts.

Civil aviation was responsible for 5.1% of US Gross Domestic Product in 2014. Over 1 billion passengers were carried by airlines operating in US airspace in 2018. The Federal Aviation Administration (FAA) estimates the cost of delay in 2018 is 28.2 billion dollars [1]. Moreover, in the next two decades, it is forecasted that each year system traffic will increase by around 2 percent, the number of aircraft in the U.S. commercial fleet will increase by around 0.9 percent, and commercial FAA operations will increase by around 1.5 percentage [2]. Therefore, air traffic flow management will only become more critical.

Traffic Management Initiatives (TMI) are tools air traffic flow managers use to balance demand with capacity in congested regions. Collaborative Trajectory Options Programs (CTOP) is the latest tool in the FAA's NextGen portfolio and the most powerful one. CTOP combines multiple features from its forerunners including Ground Delay Program (GDP), Airspace Flow Program (AFP) and reroutes, and has two important new features: first, it can manage multiple constrained regions in an integrated way with a single program; second, it allows flight operators to submit a set of desired reroute options (called a Trajectory Options Set or TOS), which provides great flexibility and efficiency. Since CTOP can be used to managed both airport and en route airspace regions, GDP and AFP can be seen as special cases of CTOP. Since CTOP can manage more than one congested region, it can replace the usage of multiple GDPs and AFPs, and avoid coordinating multiple programs [3]. There are many applications to which CTOP can be applied, but GDP and AFP are not capable to do, for example, corner post management [4] and Integrated Demand Management [5].

1.2 Research Motivation

CTOP has been deployed by the FAA since March 22, 2014. However, both FAA and airline companies are a little overwhelmed by CTOP's flexibility and complexity, and CTOP has been rarely used so far. In fact, CTOP is in a dilemma: neither FAA nor airlines are adopting CTOP, because the other side is not adopting CTOP.

On the FAA side, CTOP usage is stalled by the lack of airline participation, since there is no TOS submission. There is very little historical data available, and air traffic managers do not have experience implementing CTOP. More importantly, there are very few guidelines and is lack of decision

support tools for where to create Flow Constrained Areas (FCAs), how to set flow rates, when to do the revision, etc.

On the airline side, major companies have been hesitating in developing in-house TOS/CTOP software, because CTOP is not being used by the FAA. Airlines concern about increased workload in their dispatch department and are in doubt of the return on the investment because there have been few convincing and successful examples.

From the perspective of the development of air traffic flow management, CTOP is a natural progression of GDP and AFP. FAA and airline sides CTOP and its related research problems have to be solved sooner or later and they are inevitable. This paper primarily aims to address one of key challenges that air traffic managers face: how to set traffic flow rates for multiple FCAs in an optimal and integrated fashion, so as to help CTOP accelerate adoption at least on the FAA side.

1.3 Research Objectives

The research objectives of this paper include:

1. Understand the characteristics of airspace capacity uncertainty caused by weather forecast and traffic demand uncertainty induced by reroute options; decide the appropriate decision making under uncertainty framework
2. Understand the key differences between CTOP and classic TMIs; borrow modeling ideas from existing TMI flow rate optimization work
3. **Problem 1:** assume route choice of each flight is known (e.g. the most preferred route), how to optimize traffic flow rates to minimize system ground and air delay costs? The result itself is meaningful since it is the solution to multiple congestion regions traffic flow management problem (no reroute), which itself can be considered as a TMI, too
4. **Problem 2:** given TOS of each flight, how to optimize reroute, ground and air delay for each flight in a centralized way? The solution can tell us the theoretical system cost lower bound that can be potentially achieved, gives the traffic flow picture in the ideal scenario and is particularly useful for airline to do internal CTOPs
5. **Problem 3:** how to optimize FCA planned acceptance rates under traffic demand and airspace capacity uncertainties? This is the core question that we want to answer and the solution can directly help FAA air traffic managers to improve the implementation of CTOP programs

This paper is organized as follows: in section 2, decision making under uncertainty techniques, related literature on TMI rate optimization and weather models are reviewed, which help us achieve the first two research objectives. In section 3, three aggregate stochastic models are proposed to address the third research objective. These models can be used for both optimization and simulation purposes. In section 4, six disaggregate stochastic models are formulated to accomplish the fourth objective, which generalize a notable strong deterministic flight-by-flight level traffic flow formulation and three of them are based on aggregate models introduced in section 3. In section 5, simulation-based optimization and stochastic programming methods are combined to tackle the fifth objective and the core problem: setting traffic flow rate under demand and capacity uncertainties that are compatible with CDM-CTOP software. In section 6, the contributions are summarized, model extension and other future work are pointed out.

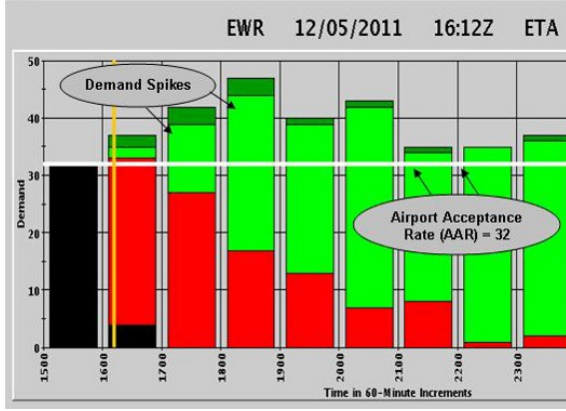


Figure 1: Demand Spikes Need to be Leveled Off

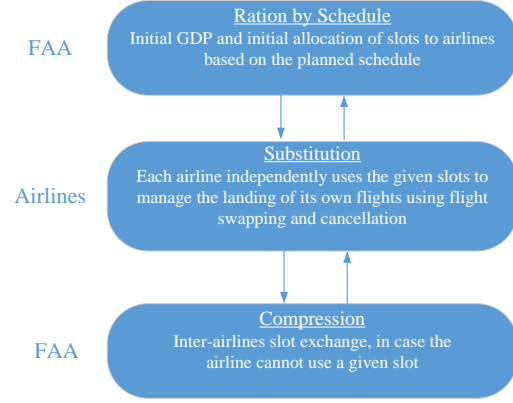


Figure 2: GDP in CDM Environment: Information Exchange Improves Efficiency while Ensuring Equality

2 Literature Review

2.1 Air Traffic Flow Management

2.1.1 Ground Delay Program

The first classic Traffic Management Initiative (TMI) is the Ground Delay Program (GDP), which was introduced in the late 1980s. It is a terminal TMI and directly impacts arrivals into a particular airport. In a GDP, flights are ground held at their departure airports because the projected demand is expected to exceed the capacity in their arrival airport for a sustained period. The idea behind the GDP is that it is cheaper and safer to hold a flight on the ground at its origin airport than to let it takeoff and subject to air delay and landing difficulties at its destination airport. Air delay is more expensive because of fuel and other operating costs [6][7][8].

Figure 1 shows the number of scheduled arrival flights to Newark airport (EWR). Different colors refer to different status of flights, e.g., flights that have already landed, flights that have taken off and have not landed yet, etc. The white line shows the airport hourly capacity. It can be seen that flight demand will exceed capacity for several hours. In this case, GDP is necessary and some flights will be ground delayed.

A key concept in TMI planning is called planned acceptance rates, which are the maximum numbers of flights that are planned to be admitted to a constrained airport or a FCA in each time period. The related concept is actual acceptance rates, which are the actual numbers of flights that land at the airport or traverse the FCA. Planned acceptance rates are control decisions made by the FAA. Actual acceptance rates are the results of the control decisions.

In a GDP, the FAA will set airport planned acceptance rates, create evenly distributed slots based on the rates, and assign these slots to GDP affected flights. A fundamental problem is how to assign slots to flights in a fair way. In the Collaborative Decision Making (CDM) environment (Figure 2), slots are allocated to the air carriers according to their original schedule, which is known as the Ration By Schedule rule or RBS. According to RBS, flights are prioritized according to their original scheduled times, even if they are delayed or cancelled. The RBS eliminates the concern of the air carrier of being penalized if they report their latest information regarding their schedule. After the arrival slots are allocated to the air carriers, each air carrier can independently reorganize and swap its own flights into its own slots. This step, known as substitution, allows the air carrier to reduce the delay of its important flights and take advantage of the empty slots of cancelled flights. The last step in CDM-GDP is compression. It is used to fill in the landing slots that are cannot used by some air carriers, which will benefit all air carriers [9][10][11].

2.1.2 Airspace Flow Program

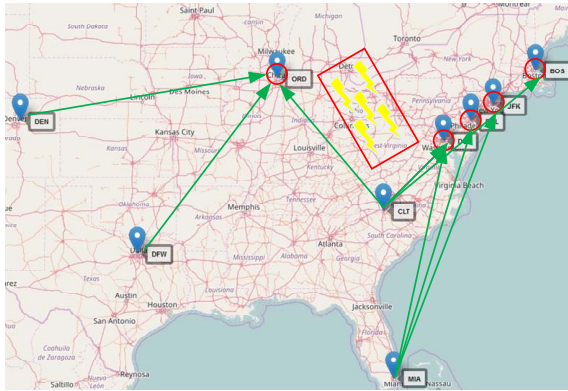


Figure 3: GDP is Inefficient When Dealing With En route Constraint

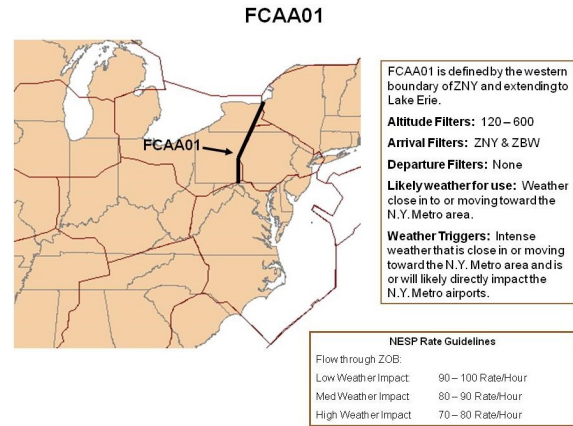


Figure 4: A FCA Locates at the boundary of New York Air Route Traffic Control Center (ZNY ARTCC)

The second classic TMI is the Airspace Flow Program (AFP), which was introduced in summer 2006. AFP is an enroute TMI, which is used to manage air traffic in the en route segment of flight. The initial implementation of strategic air traffic flow management was primarily focused on airports. However, later it was found that significant flight delays and system degradations are due to en route airspace problems, particularly from convective weather activity and demand surges. Before AFP was introduced, to cope with severe convective weather and reduce the en route demand through constrained airspace, air traffic managers would implement GDPs at multiple major airports to reduce flows of traffic to these airports (Figure 3). This approach is very inefficient because it may delay flights that do not directly contribute to problem and assign no delay to flights that traverse the constrained airspace [12][13][14].

In AFP, the en route airspace can be directly managed using a concept called Flow Constrained Area (FCA), which controls the traffic flow into the congested airspace region (Figure 4).

In both GDP and AFP, there is only one constrained resource is involved and each flight only has one route option.

2.1.3 Collaborative Trajectory Options Program

The latest TMI is called Collaborative Trajectory Options Program (CTOP), which was deployed in March, 2014. CTOP combines multiple features from its forerunners, including GDP, AFP and required reroutes, and can manage multiple FCAs with a single program. The most important concept in CTOP is Trajectory Options Set or TOS. TOS is a set of desired reroute option submitted by flight operators. Using TOS, the flight operator can now express their preferences in terms of delay on the ground versus longer flying time. In the past, if a constraint has been identified, air traffic managers will either assign a delay (by way of AFP) or specify a reroute. In CTOP, the FAA will set the FCA planned acceptance rates and let the flight operators to decide which they would prefer: a ground delay, a reroute or a combination of both.

Table 1 shows an example of a TOS. A TOS consists of a flight's ID, origin and destination airports, Initial Gate Time of Departure (IGTD, the departure time when the flight was first created), Earliest Runway Time of Departure (ERTD, the earliest time the flight can depart) and candidate routes information.

Relative Trajectory Costs (RTCs) are values submitted by the flight operator to express his/her preference over route options. There are three optional requirements for each route that can be provided by flight operator: Required Minimum Notification Time (RMNT) which allows for needed preparation time, such as adding fuel; Trajectory Valid Start Time (TVST) and Trajectory Valid

End Time (TVET) which are the earliest and latest acceptable take-off times for that TOS option, respectively.

Table 1: TOS Example of a Flight from LAX to ATL

Flight ID					
ACID	ORIG	DEST	IGTD	TYPE	ERTD
ABC123	LAX	ATL	05/1945	LJ60	05/1945

Trajectory Option Set						
RTC	RMN T	TVS T	TVE T	Route	ALT	SPEED
0				TRM PKE DRK J6 IRVV FSM MEM ERLIN9	350	435
30			2045	TRM PKE DRK J134 LBL SGF BNA RMG4	350	435
50		2045		TRM PKE DRK J134 BUM FAM BNA RMG4	350	430
60		1945	2145	TRM BLH J169 TFD J50 SSO J4 EWM J66 ABI J4 MEI LGC2	350	425
70	45	1745	2200	TRM BLH J169 TFD ELP J2 JCT J86 IAH J2 LCH J590 GCV LGC2	310	430

FAA allocates the routes to flights on a flight basis according to their earliest Initial Arrival Times (IATs). A flight's IAT is the earliest ETA (Estimated Time of Arrival) at any of a CTOP's FCAs using any of this flight's TOS options. We can consider IAT as a flight's CTOP capture time. This is the CTOP version of Ration by Schedule (RBS). For a given flight, CTOP allocation algorithm will

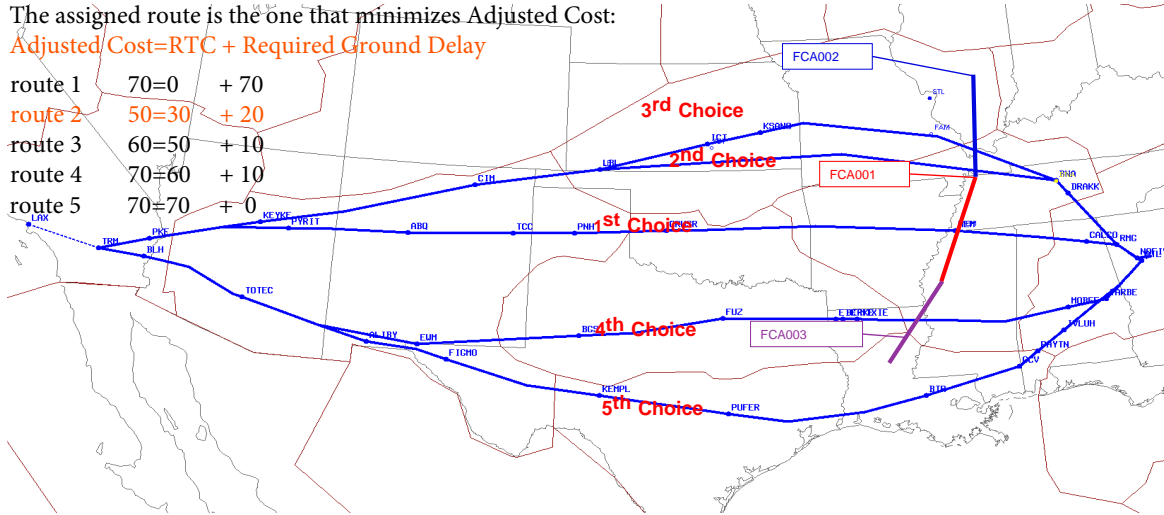


Figure 5: Flight Routes in the TOS and the Adjusted Cost

calculate the adjusted cost for each candidate route and assign the route with the minimum adjusted cost to this flight. The key equation here is:

$$\text{Adjusted Cost} = \text{RTC} + \text{Required Ground Delay} \quad (1)$$

Required ground delay is calculated by the CTOP algorithm given current available slots, which is the ground hold time this flight will need to bear in order to take a specific route. Assume no route restriction is violated, as shown in Figure 5, this flight will be allocated with route 2, which has the smallest adjusted cost among all route options.

The three optional route restrictions may also affect the route assignment. The scheduled departure time of this flight is 19:45. Assume the current time is 19:10. The RMNT dictates that if route 5 is chosen, then this flight cannot depart until 19:10 + 45 mins = 19:55. In this case the required ground delay is actually 10 minutes and the adjusted cost is 80 minutes. It can be seen that apart from available slots, the route restrictions can be another source for required ground delay. For route 3, the flight needs to take 60 minutes ground delay in order to meet the TVST requirement: 19:45 + 60 mins = 20:45. Therefore if the route restriction is considered, the adjusted cost for route 3 is 110 minutes. Route 2 still has the smallest the adjusted cost and satisfies TVET: 19:45 + 20 mins = 20:05 ≤ 20:45.

For a more detailed introduction to CTOP algorithm, the readers are referred to [15] or [16].

Since CTOP can be used to manage both terminal and en route airspace regions, therefore GDP and AFP can be seen as special cases of CTOP. Since CTOP comprises multiple FCAs and each flight has a TOS, CTOP traffic flow rates planning is multiple constrained regions multiple reroutes planning problem.

2.1.3.1 TOS-induced Demand Uncertainty

In previous sections we have introduced that in CTOP, FAA will set acceptance rates for each FCA, then run TOS allocation algorithm to assign slots to CTOP captured flights. Therefore only after finishing these two steps, air traffic managers can know which route each flight will take. Demand uncertainty refers to the problem that when setting FCA flow rates, air traffic managers do not know which route in a flight's TOS will be assigned to this flight, thus traffic demand for each constrained region is uncertain. This new source of uncertainty is brought by the introduction of TOS, thus it is called TOS-induced demand uncertainty or demand variability.

2.1.4 Weather Translation Models

Airport and airspace capacity is the key parameter in air traffic flow management models. To prepare this parameter for deterministic optimization models, weather translation model is used by the FAA to compute capacity reduction factor or quantile. The capacity of adverse weather impacted region is then the nominal capacity times reduction factor.

Translating ensemble weather forecasts to probabilistic capacity information is an important line of research in the aviation weather community [17, 18, 19]. There are two representative works that study how to generate scenario tree from weather data. In [20], historical weather data is used and two steps approach is employed: clustering method is first used to develop scenarios, then a heuristic method is used to assemble scenarios into a tree by finding the branching points. In [21], hierarchical clustering approach is used to generate capacity scenarios from weather forecasts. The result is a scenario bush.

2.2 Decision Making Under Uncertainty Approaches

CTOP rates planning is a decision making under uncertainty problem. Here we review several frameworks related to decision making under uncertainty problems.

2.2.1 Deterministic Mixed Integer Linear Programming Model (MILP)

In deterministic model, we assume all model parameters are perfectly known. Deterministic model is the basis for decision making uncertainty models.

There are two paradigms of deterministic air traffic flow management models: *Lagrangian* models, which work at a flight-specific level and provide trajectories and departure times for each flight, and *Eulerian* models, which work at the aggregate flow-based level and provide counts of aircraft in airspace regions. The main advantage of Lagrangian models is their flexibility and ability to cope with flight-specific differences. Though these models tend to be NP-hard, it has been shown that by carefully picking decision variables, a strong formulation can possibly be obtained and realistic-size problem instances can be solved [22, 23, 24]. The advantages of Eulerian models are that they depend only on the size of the geographic regions of interest rather than on the number of aircraft in the regions, and they have structure which facilitates the use of classic control theories [25, 26, 27, 28, 29].

2.2.2 Stochastic Programming

As mentioned in [30], one of the first applications of stochastic programming was done by George Dantzig to allocation aircraft to routes as early as 1956. That problem belongs to airline operation.

Two pioneering works on applying two-stage and multistage stochastic programming to GDP problem were done by Richetta et al. in the early 1990s [31, 32]. The first stochastic model that conforms

to the current CDM operating procedure, proposed by Ball et al. [33], is a two-stage highly aggregate model that directly computes planned acceptance rates for a weather-impacted airport. It was later proved that under mild conditions, the model in [31] can also generate CDM-compatible solutions [34]. In the aforementioned models, once a ground-delay decision is made, it cannot be revised, even if the flight is still on the ground and further ground-holding is possible. Mukherjee formulated a disaggregate multistage model that allows a flight to take ground delays multiple times based on the latest capacity information and the scenario tree structure [35]. Importantly, his model gives the theoretical lower bound on system cost for the scenario-based GDP planning problem. In this paper, we will generalize these models in several ways to solve CTOP related planning problems.

2.2.3 Robust Optimization

In robust optimization, we assume uncertainty parameters are contained in an uncertainty set. A robust feasible solution needs to satisfy all realizations of the constraints from the uncertainty set [36]. There are two papers that apply robust optimization to solve air traffic flow management problems [37, 38]. Both works deal with capacity uncertainty and use a specific weather assumption. To address the over-conservative issue, two-stage and multistage robust optimization models are formulated [39].

2.2.4 Chance Constrained Programming

In chance-constrained optimization, we optimize objective function while controlling the probability that a constraint is violated. There are three representative works of using chance constrained programming to solve air traffic flow management problems. In [40], the authors formulated an integer programming problem, which can quickly become intractable as the problem size increases. In [41] used historical weather data, adopted log-concave weather distribution assumption, applied branch and bound and first order method to solve integer convex optimization problem. In [42], the authors applied quantile estimate to get airport capacity, which approximately has the same effect as chance constraint.

2.2.5 Markov Decision Process

Researchers have explored using Markov Decision Process (MDP) in GDP flow rates planning [43, 44, 45]. The first problem with these MDP models is that it takes a long time to solve, even with approximate dynamic programming techniques. The bigger problem with applying MDP approach to CTOP is that, like in robust optimization and chance constrained programming, the weather assumption is a little too restrictive.

2.2.6 Machine Learning (Data-driven) Approach

Machine learning techniques can be applied to find similar days in the NAS, and past decisions are used as references for human decision makers [46, 47, 48, 49]. This could reduce the inconstancy of the decisions. This is not applicable for CTOP, because we do not have historical data for CTOP.

2.2.7 Simulation-based Optimization

Simulation-based approach has also been used to in air traffic flow management, for example, in determining the GDP parameters under uncertainty [50] and in strategically selecting TMI combinations [51].

3 Aggregate Stochastic Models

3.1 Introduction

In the section, we start off simple and address problem 1 listed in section 1.3. Problem 1 can be seen as a subproblem of problem 3, since demand uncertainty issue does not need to be considered. This is a FAA side research problem, therefore we care about minimizing system-wide ground and air delay costs. The goal is to optimize CTOP traffic flow rates, which means we want to optimally control the number of flights to be accepted to each constrained region in each time period. Because there are now multiple congested airspace regions, the traffic flows need to be managed in an integrated way.

In this section, we first introduce several important concepts that will be used through out this work. We emphasize that CTOP planning problem is essentially a multi-commodity flow problem. Next, we list the model assumptions, discuss in detail the three aggregate stochastic models and some additional modeling considerations. After that, we will talk about the experiment setup and discuss the numerical results. In the end, we summarize the findings.

3.2 Preliminary Concepts

3.2.1 Potentially Constrained Area (PCA) and Capacity Scenarios

In this work, a constrained airspace resource is modeled as a Potentially Constrained Area (PCA), in which air traffic demand may exceed capacity and whose future capacity realization is represented by a finite set of scenarios arranged in a scenario tree. A related concept is the PCA network, which refers to a directed graph that links the PCAs and models the potential movement of traffic between them. Figure 6 shows the scenario tree used in this work. Scenarios 1 to 3 correspond to optimistic, average and pessimistic weather forecasts, respectively. Figure 7 shows an example of PCA network that is composed of three en route PCAs and one constrained airport EWR. In multi-resource air traffic management problem, the change of operating condition at any PCA will result in a branch point in the scenario tree. Therefore, scenario tree in Figure 6 models the evolution of the future capacities of all four PCAs in Figure 7.

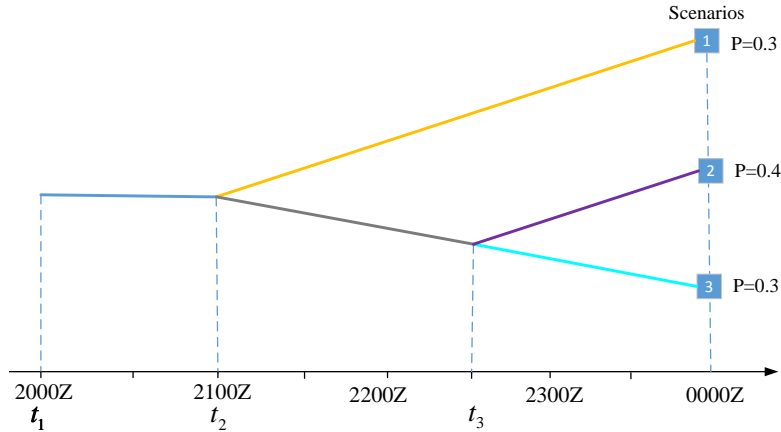


Figure 6: Scenario Tree of PCAs' Evolving Capacities

3.2.2 Path, Direct Demand and Upstream Demand

One key characteristic of general multi-resource air traffic management is that the problem is in nature a multi-commodity problem, since flights will traverse different congested airspace and reach different destinations. One the other hand, even though there may be several constrained resources involved, single airport ground hold and reroute model is essentially a single commodity problem, since all air traffic is bound for the same destination [52].

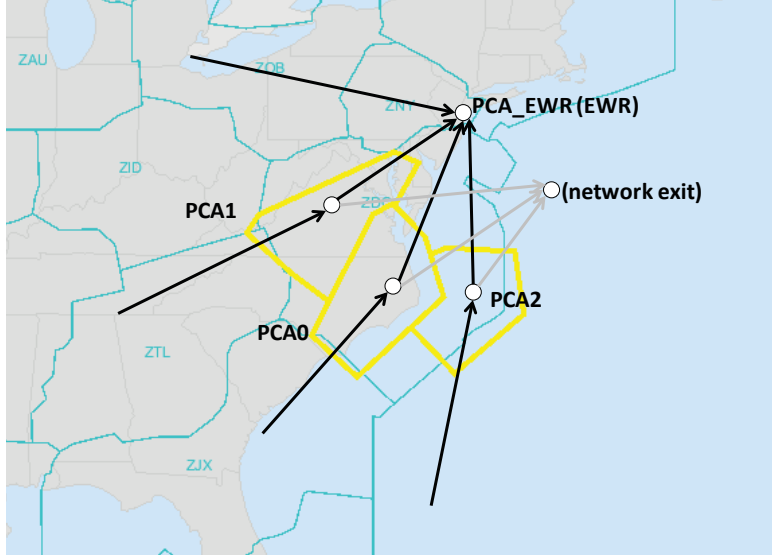


Figure 7: Geographical Display of a PCA Network

In a PCA network, flights are grouped by “path”, which is the sequence of PCAs that flights traverse. A path uniquely determines a commodity in the multi-commodity flow model. For example, in Figure 7, $\text{PCA1} \rightarrow \text{PCA_EWR}$ is one path and $\text{PCA1} \rightarrow \text{PCA_Exit}$ is another path. Flights in these two paths share the capacity resource of PCA1.

We differentiate direct demand, which are the flights flying from departing airports, with upstream demand, which are the flights flying from the upstream en route PCA. We can ground hold direct demand before flights taking off, and we can air hold both direct demand and upstream demand. Since flights are grouped by path, a flight will enter the PCA network through the first PCA (denoted as ρ_1) on its path ρ and exit through the last PCA (denoted as ρ_{-1}) on its path. For example, for path $\text{PCA1} \rightarrow \text{PCA_EWR}$, $\rho_1 = \text{PCA1}$, $\rho_{-1} = \text{EWR}$.

3.3 Model Assumptions

Several assumptions are made in this work. Firstly, the TOS route information, the topology of the PCA network, unimpeded PCA entry times, CTOP start and end times, and scenario-based PCA capacity information are given as model inputs. In this section, each flight is assumed to take the shortest route in its TOS set. Secondly, all flights are required to exit the PCA network by the end of the planning horizon. This boundary condition ensures that results from different models can be fairly compared. Thirdly, the planning horizon is equally divided into 15-minute time periods.

3.4 Two-stage Static Model

Two-stage aggregate stochastic model is introduced in this section. In this model, the first stage decisions are the ground delays assigned to the flights. The second stage decisions are the air delays the flights need to take in response to the realization of the weather scenarios. This model is an explicit multi-commodity flow model, since every decision variable has subscript ρ , which represents path (commodity).

Direct demand can be ground delayed. At the first PCA on each path, we have the following relationship for planned acceptance rates, originally scheduled arrival demand and ground delays:

$$P_{t,\rho}^k = D_{t,\rho}^k - (G_{t,\rho}^k - G_{t-1,\rho}^k) \quad \forall t \in \mathcal{T}, \rho \in \mathcal{P}, k = \rho_1 \quad (2)$$

If k is the first PCA on that path, the actual demand at PCA k on path ρ in time period t will be $P_{t,\rho}^k$. Otherwise, the actual demand will be the number of flights from upstream PCA which is scenario

dependent $\text{UpPCA}_{t,\rho}^{k,q}$. For each case we have:

$$L_{t,\rho}^{k,q} = \begin{cases} \text{if } k = \rho_1 & P_{t,\rho}^k - (A_{t,\rho}^{k,q} - A_{t-1,\rho}^{k,q}) \\ \text{else} & \text{UpPCA}_{t,\rho}^{k,q} - (A_{t,\rho}^{k,q} - A_{t-1,\rho}^{k,q}) \end{cases} \quad \forall t \in \mathcal{T}, q \in \mathcal{Q}, \rho \in \mathcal{P}, k \in \rho \quad (3)$$

$$\text{UpPCA}_{t,\rho}^{k,q} = L_{t-\Delta^{k',k},\rho}^{k',q} \quad \forall t \in \mathcal{T}, q \in \mathcal{Q}, (k', k) \in \rho \quad (4)$$

Constraint (3) enforces the number of flights which actually cross PCA k equals to the actual demand minus the incremental number of flights taking air delay. Constraint (4) stipulates that, when calculating the traffic demand at k from the upstream PCA k' , the average travel time between (k, k') needs to be considered. In the $\text{PCA1} \rightarrow \text{PCA_EWR}$ path example, the first case in (3) corresponds to PCA1 and the second case corresponds to PCA_EWR .

Remarks: constraints (2) and (3) characterize the most important tradeoff in the model: if scheduled traffic flow rates are smaller than the demand, then some flights will need to take ground delay; if scheduled traffic flow rates are greater than the actual capacities of the constrained regions, flights will have to take more expensive air delay.

Different groups of traffic flows are coupled through the capacity constraints at their shared PCAs:

$$\sum_{\rho \in \mathcal{P}} L_{t,\rho}^{k,q} \leq M_{t,q}^k, \quad \forall t \in \mathcal{T}, q \in \mathcal{Q}, k \in \mathcal{P} \quad (5)$$

All the decision variables are required to be nonnegative integers:

$$P_{t,\rho}^k, G_{t,\rho}^k, L_{t,\rho}^{k,q}, A_{t,\rho}^{k,q} \in \mathbb{Z}_+ \quad \forall t \in \mathcal{T}, q \in \mathcal{Q}, \rho \in \mathcal{P}, k \in \rho \quad (6)$$

Boundary conditions are needed in air traffic management models to guarantee all flights are properly handled, so that we can fairly compare the performance of different models. It is worth noting that the following boundary condition, which is used in GDP models [33], cannot ensure all flights will land at the end of the planning horizon in the multiple constrained resources case:

$$G_{0,\rho}^k = A_{|\mathcal{T}|,\rho}^k = 0 \quad \forall \rho \in \mathcal{P}, k \in \rho \quad (7)$$

The reason is that in multiple resources case, it takes time to travel from one resource to a downstream resource. Even though there is no ground or air held flight, there can still be flights in the PCA network because of $L_{t,\rho}^{k,q}$. If we want all the flights to land/exit the PCA network by the last time period, we will need to explicitly enforce, for each path and for each scenario, the total scheduled demand of flights belonging to path ρ equals to the cumulative number of flights which exits the PCA system via the last PCA on path ρ :

$$\sum_{t \in \mathcal{T}} D_{t,\rho}^{k=\rho_1} = \sum_{t \in \mathcal{T}} L_{t,\rho}^{k=\rho-1,q} \quad \forall q \in \mathcal{Q}, \rho \in \mathcal{P} \quad (8)$$

There are several performance metrics for evaluating a TMI. The three most important metrics are efficiency, equity and capacity utilization [53, 54]. In this model, like most other air traffic flow management models in the literature, the objective function minimizes the ground delay and (expected) air delay cost:

$$\min \quad c_g \sum_{t \in \mathcal{T}} \sum_{\rho \in \mathcal{P}} G_{t,\rho}^{k=\rho_1} + c_a \sum_{q \in \mathcal{Q}} p_q \sum_{t \in \mathcal{T}} \sum_{\rho \in \mathcal{P}} \sum_{k \in \rho} A_{t,\rho}^{k,q} \quad (9)$$

3.5 Multistage Semi-Dynamic Model

A drawback of the static model is that we do not take advantage of the updated weather information or the structure of a scenario tree. In this section, the multistage semi-dynamic stochastic model is introduced, which could partially overcome this limitation. In this model, for each flight the ground delay decision is no longer made at the beginning of the planning horizon, instead it is made at

some pre-determined time before scheduled departure time, e.g., at the beginning of a flight' original scheduled departure stage. The model is named semi-dynamic because compared with the model which will be introduced in the next section, the ground delay, once assigned, cannot be revised and thus the model is not fully dynamic.

In this model, the concept of stage is used. A stage can comprise several time periods, in which we have the same weather information. For example, in Figure 6 there are three stages, and the dotted vertical lines indicate the starting times of each stage. Like in the previous section, we will plan ground delay for the scheduled direct demand. A new primary decision variable $X_{s,t,t',\rho}^{k,q}$ is used, which records not only the originally scheduled arrival time, but also originally scheduled departure stage. For the first PCA on each path, we have the following conservation of flow constraints:

$$\sum_{t'=t}^{|\mathcal{T}|} X_{s,t,t',\rho}^{k,q} = S_{s,t,\rho}^k \quad \forall s \in \mathcal{S}, t \geq t_s, q \in \mathcal{Q}, \rho \in \mathcal{P}, k = \rho_1 \quad (10)$$

For variable $X_{s,t,t',\rho}^{k,q}$, we must have $t' \geq t \geq t_s$. Variable $X_{s,t,t',\rho}^{k,q}$ contains the ground delay information. From $X_{s,t,t',\rho}^{k,q}$ we can calculate the actual direct demand at the first PCA k on path ρ in each time period, which is now scenario dependent:

$$P_{t,\rho}^{k,q} = \sum_{\substack{s \in \mathcal{S} \\ t \geq t_s}} \sum_{t' \geq t'} X_{s,t',t,\rho}^{k,q} \quad \forall t \in \mathcal{T}, q \in \mathcal{Q}, \rho \in \mathcal{P}, k = \rho_1 \quad (11)$$

The other constraints are similar to the static model:

$$L_{t,\rho}^{k,q} = \begin{cases} \text{if } k = \rho_1 & P_{t,\rho}^{k,q} - (A_{t,\rho}^{k,q} - A_{t-1,\rho}^{k,q}) \\ \text{else} & \text{UpPCA}_{t,\rho}^{k,q} - (A_{t,\rho}^{k,q} - A_{t-1,\rho}^{k,q}) \end{cases} \quad \forall t \in \mathcal{T}, q \in \mathcal{Q}, \rho \in \mathcal{P}, k \in \rho \quad (12)$$

$$\text{UpPCA}_{t,\rho}^{k,q} = L_{t-\Delta^{k',k},\rho}^{k',q} \quad \forall t \in \mathcal{T}, q \in \mathcal{Q}, (k', k) \in \rho \quad (13)$$

$$\sum_{\rho \in \mathcal{P}} L_{t,\rho}^{k,q} \leq M_{t,q}^k \quad \forall t \in \mathcal{T}, q \in \mathcal{Q}, k \in \mathcal{P} \quad (14)$$

$$X_{s,t,t',\rho}^{k,q} \in \mathbb{Z}_+ \quad \forall s \in \mathcal{S}, t \geq t_s, q \in \mathcal{Q}, \rho \in \mathcal{P}, k = \rho_1 \quad (15)$$

$$P_{t,\rho}^{k,q}, L_{t,\rho}^{k,q}, A_{t,\rho}^{k,q} \in \mathbb{Z}_+ \quad \forall t \in \mathcal{T}, q \in \mathcal{Q}, \rho \in \mathcal{P}, k \in \rho \quad (16)$$

$$A_{0,\rho}^{k,q} = 0 \quad \forall q \in \mathcal{Q}, \rho \in \mathcal{P}, k \in \rho \quad (17)$$

$$\sum_{s \in \mathcal{S}} \sum_{t \geq t_s} S_{s,t,\rho}^{k=\rho_1} = \sum_{t \in \mathcal{T}} L_{t,\rho}^{k=\rho-1,q} \quad \forall q \in \mathcal{Q}, \rho \in \mathcal{P} \quad (18)$$

For multistage model, we have the set of nonanticipativity constraints, which ensure that decisions made in time period t are solely based on the information available at that time .

$$X_{s,t,t',\rho}^{k,q_1^b} = \dots = X_{s,t,t',\rho}^{k,q_{N_b}^b} \quad \forall \rho \in \mathcal{P}, k = \rho_1, s \in \mathcal{S}, t \geq t_s, t' \geq t, b \in \mathcal{B}, t_s \in b \quad (19)$$

This set of constraints mean that if a set of scenarios are on the same branch, we should take exactly the same actions with respect to this set of scenarios. The branch(es) information is determined by s , the original scheduled departure time. For example, if we are at time period $t_1 + 1$ (stage 2), we should impose:

$$X_{2,t_1+1,t',\rho}^{k,2} = X_{2,t_1+1,t',\rho}^{k,3} \quad \forall \rho \in \mathcal{P}, k = \rho_1, t' \geq t_1 + 1 \quad (20)$$

The objective function minimizes the expected ground delay and air delay cost:

$$\min \sum_{q \in \mathcal{Q}} p_q \left(\sum_{s \in \mathcal{S}} \sum_{\substack{t'=t \\ t \geq t_s}}^{|\mathcal{T}|} \sum_{\rho \in \mathcal{P}} c_g(t' - t) X_{s,t,t',\rho}^{k,q} + \sum_{t \in \mathcal{T}} \sum_{\rho \in \mathcal{P}} \sum_{k \in \rho} c_a A_{t,\rho}^{k,q} \right) \quad (21)$$

Remarks: since semi-dynamic model is more flexible than static model, one would suspect static model is a special case of semi-dynamic model. In fact, if we impose the nonanticipativity constraints at the root of the scenario tree, semi-dynamic model will produce exactly the same result as the static model:

$$X_{s,t,t',\rho}^{k,1} = X_{s,t,t',\rho}^{k,2} = \dots = X_{s,t,t',\rho}^{k,|\mathcal{Q}|} \quad \forall \rho \in \mathcal{P}, k = \rho_1, s \in \mathcal{S}, t \geq t_s, t' \geq t \quad (22)$$

3.6 Multistage Dynamic Model

In this section, the fully dynamic model is introduced. The key idea of this model is that when making ground delay decisions, we will consider the possibility this flight may be further ground delayed later on ("plan to replan").

One major difference between this model with the previous two models is that we will group flights not only by path but also by en route time. This is because in a fully dynamic model, the nonanticipativity constraints will be enforced at a flight's actual departure time. We need to know, if we let these flights take off now, how long it will take for these flights get into the PCA network and become real demands to the PCAs.

Different from two-stage static model, where we have conservation of flow constraints at the first PCA on each path, here conservation of flow constraints are imposed at departure airports for all groups of flights:

$$P_{t,l,\rho}^{k,q} = D_{t,l,\rho}^k - (G_{t,l,\rho}^{k,q} - G_{t-1,l,\rho}^{k,q}) \quad \forall t \in \mathcal{T}, l \in \mathcal{L}, \rho \in \mathcal{P} \quad (23)$$

$P_{t,l,\rho}^{k,q}$ now is the *planned release rate*, rather than the planned acceptance rate. $D_{t,l,\rho}^k$ is the scheduled departure demand, instead of the scheduled arrival demand as in two-stage static model. The direct demand for PCA k in time period t from flights with the same path ρ under scenario q is:

$$\sum_{l \in \mathcal{L}} P_{t-l,l,\rho}^{k,q} \quad (24)$$

The other constraints are similar to static and semi-dynamic models:

$$L_{t,\rho}^{k,q} = \begin{cases} \text{if } k = \rho_1 & \sum_{l \in \mathcal{L}} P_{t-l,l,\rho}^{k,q} - (A_{t,\rho}^{k,q} - A_{t-1,\rho}^{k,q}) \\ \text{else} & \text{UpPCA}_{t,\rho}^{k,q} - (A_{t,\rho}^{k,q} - A_{t-1,\rho}^{k,q}) \end{cases} \quad \forall t \in \mathcal{T}, q \in \mathcal{Q}, \rho \in \mathcal{P}, k \in \rho \quad (25)$$

$$\text{UpPCA}_{t,\rho}^{k,q} = L_{t-\Delta^{k'},k,\rho}^{k',q} \quad \forall t \in \mathcal{T}, q \in \mathcal{Q}, (k', k) \in \rho \quad (26)$$

$$\sum_{\rho \in \mathcal{P}} L_{t,\rho}^{k,q} \leq M_{t,q}^k \quad \forall t \in \mathcal{T}, q \in \mathcal{Q}, k \in \mathcal{P} \quad (27)$$

$$P_{t,l,\rho}^{k,q}, G_{t,l,\rho}^{k,q}, L_{t,\rho}^{k,q}, A_{t,\rho}^{k,q} \in \mathbb{Z}_+ \quad \forall t \in \mathcal{T}, l \in \mathcal{L}, q \in \mathcal{Q}, \rho \in \mathcal{P}, k \in \rho \quad (28)$$

$$G_{0,l,\rho}^{k,q} = A_{0,\rho}^{k,q} = 0 \quad \forall l \in \mathcal{L}, q \in \mathcal{Q}, \rho \in \mathcal{P}, k \in \rho \quad (29)$$

$$\sum_{t \in \mathcal{T}} \sum_{l \in \mathcal{L}} D_{t,l,\rho}^{k=\rho_1} = \sum_{t \in \mathcal{T}} L_{t,\rho}^{k=\rho-1,q} \quad \forall q \in \mathcal{Q}, \rho \in \mathcal{P} \quad (30)$$

As has been emphasized, the nonanticipativity constraints are imposed at flights' actual departure time, which will determine the branch(es) information at that time:

$$P_{t,l,\rho}^{k,q_1^b} = \dots = P_{t,l,\rho}^{k,q_{N^b}^b} \quad \forall t \in \mathcal{T}, l \in \mathcal{L}, \rho \in \mathcal{P}, k = \rho_1, b \in \mathcal{B}, t \in b \quad (31)$$

Objective function minimizes the expected ground delay and air delay cost:

$$\min \sum_{q \in \mathcal{Q}} p_q \left(c_g \sum_{t \in \mathcal{T}} \sum_{l \in \mathcal{L}} \sum_{\rho \in \mathcal{P}} G_{t,l,\rho}^{k=\rho_1,q} + c_a \sum_{t \in \mathcal{T}} \sum_{\rho \in \mathcal{P}} \sum_{k \in \rho} A_{t,\rho}^{k,q} \right) \quad (32)$$



Figure 8: Weather Forecast for 2210z, Taken at 1522z on July 15, 2016

Remarks: similar to (22), we can impose the following constraint to make static model a special case of dynamic model:

$$\sum_{l \in \mathcal{L}} P_{t-l, l, \rho}^{k, 1} = \sum_{l \in \mathcal{L}} P_{t-l, l, \rho}^{k, 2} = \dots = \sum_{l \in \mathcal{L}} P_{t-l, l, \rho}^{k, |\mathcal{Q}|} \quad \forall t \in \mathcal{T}, \rho \in \mathcal{P}, k = \rho_1 \quad (33)$$

Denote $P_{t, \rho}^{k, q}$ as the solution of semi-dynamic model. By imposing the following constraints we can also recover semi-dynamic solution from dynamic model solution

$$P_{t, \rho}^{k, q} = \sum_{l \in \mathcal{L}} P_{t-l, l, \rho}^{k, q} \quad \forall t \in \mathcal{T}, \rho \in \mathcal{P}, k = \rho_1 \quad (34)$$

3.7 Experimental Results

To demonstrate the performance of the proposed models, we created an operational use case based on actual events on July 15, 2016. This use case primarily addresses convective weather activity in southern Washington Center (ZDC) and EWR airport. Figure 8 shows the pattern of convective weather activity for that day. There is a four-hour capacity reduction in ZDC/EWR from 2000z to 2359z. By analyzing the weather and traffic trajectory (Figure 9) data, we can build the PCA network, shown in Figure 7.

3.7.1 Capacity Profiles and Traffic Demand

For simplicity, in this work we directly manipulated the capacity profiles from the base forecast to create the alternate capacity profiles, which gives us full control over the capacity profiles for experimental purposes. In practice, weather translation techniques introduced in section 2.1.4 can be used to generate probabilistic weather scenario.

A relatively simple scenario tree is used, shown in Figure 6. Three scenarios correspond to the optimistic, average and pessimistic weather forecasts, respectively. This scenario tree has more than one branching point and it is expected that multistage models will take advantage of the structure information and outperform the static model. The detailed capacity information is listed in Table 2. We can see that in scenario 1 at 2100Z PCA1's 15-minute capacity changes from 44 to 50, the EWR's capacity changes from 8 to 10; in scenario 2 at 2230Z, the capacities of PCA1 and EWR return to the nominal values. These two changes correspond to the two branch points in the scenario tree shown in Figure 6.

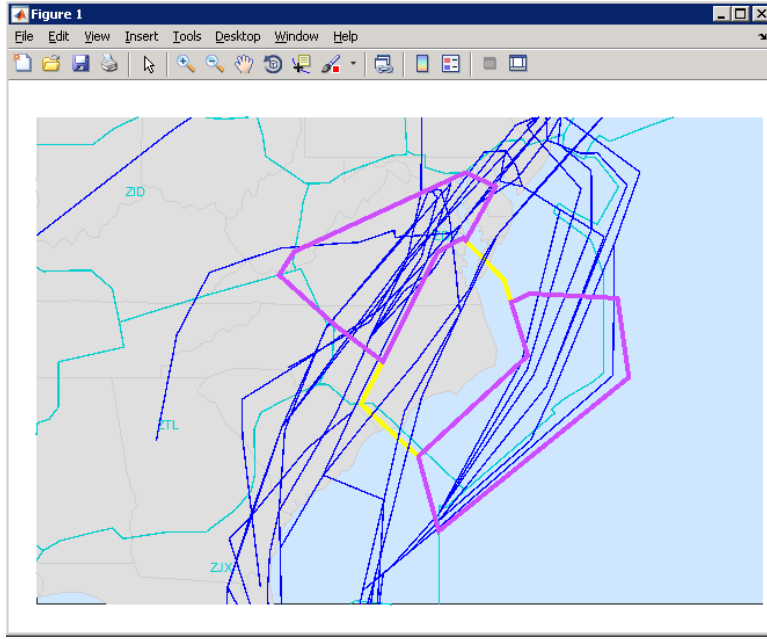


Figure 9: Traffic Routing Around the Original (Yellow) PCA

Table 2: Capacity Scenarios

Resource/Time Bin		20:00	15	30	45	21:00	15	30	45	22:00	15	30	45	23:00	15	30	45	00:00	15	30	45	01:00	15	30	45
Scen1	PCA0	13	13	13	13	25	25	25	25	25	25	25	25	25	25	25	25	25	25	25	25	25	25	25	25
	PCA1	44	44	44	44	50	50	50	50	50	50	50	50	50	50	50	50	50	50	50	50	50	50	50	50
	PCA2	5	5	5	5	5	5	5	5	5	5	5	5	5	5	5	5	5	5	5	5	5	5	5	5
	EWR	8	8	8	8	10	10	10	10	10	10	10	10	10	10	10	10	10	10	10	10	10	10	10	10
Scen2	PCA0	13	13	13	13	13	13	13	13	13	13	25	25	25	25	25	25	25	25	25	25	25	25	25	25
	PCA1	44	44	44	44	44	44	44	44	44	44	50	50	50	50	50	50	50	50	50	50	50	50	50	50
	PCA2	5	5	5	5	5	5	5	5	5	5	5	5	5	5	5	5	5	5	5	5	5	5	5	5
	EWR	8	8	8	8	8	8	8	8	8	8	10	10	10	10	10	10	10	10	10	10	10	10	10	10
Scen3	PCA0	13	13	13	13	13	13	13	13	13	13	13	13	13	13	13	13	25	25	25	25	25	25	25	25
	PCA1	44	44	44	44	44	44	44	44	44	44	44	44	44	44	44	44	50	50	50	50	50	50	50	50
	PCA2	5	5	5	5	5	5	5	5	5	5	5	5	5	5	5	5	5	5	5	5	5	5	5	5
	EWR	8	8	8	8	8	8	8	8	8	8	8	8	8	8	8	8	10	10	10	10	10	10	10	10

Note in GDP optimization, we usually add one extra time period to make sure all flights will land at the end of the planning horizon. Because CTOP has multiple constrained resources, depending on the topology of the PCA network, we need to add more than one time period. In this case, we add eight extra time periods, because the longest travel time between the three en route PCAs and EWR among all TOS options is around 2 hours (8 time periods). For any time periods outside the CTOP start-end time window, e.g. the eight extra time periods in Table 2, nominal capacities are used.

Flight trajectory data from the FAA’s System Wide Information Management (SWIM) and Coded Departure Route (CDR) databases are used for traffic demand modeling. In total 1098 flights are captured by this CTOP, among them 890 flights that traverse the PCAs in their active periods. Figure 10 to Figure 13 show the demand information at the four PCAs if no flight takes any delay.

It can be seen that from Figure 7 that there are in total 7 possible paths: direct demand to EWR, passing one of the three en route PCAs then landing at EWR or passing one of the en route PCAs then exiting the system. We require all the CTOP captured flights to land at EWR/exit the PCA network at the end of the planning horizon.

3.7.2 Model Comparisons

All optimization models are solved using Gurobi 8.1 on a laptop with 3.6 GHz processors and 32 GB RAM. The main results are listed in Table 3. There are some key observations from this table:

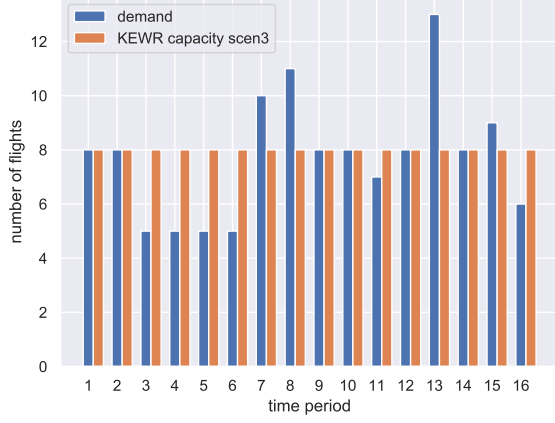


Figure 10: Demand and Capacity at EWR

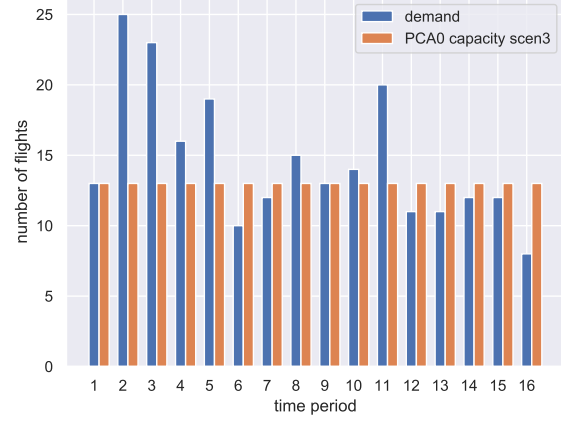


Figure 11: Demand and Capacity at PCA0

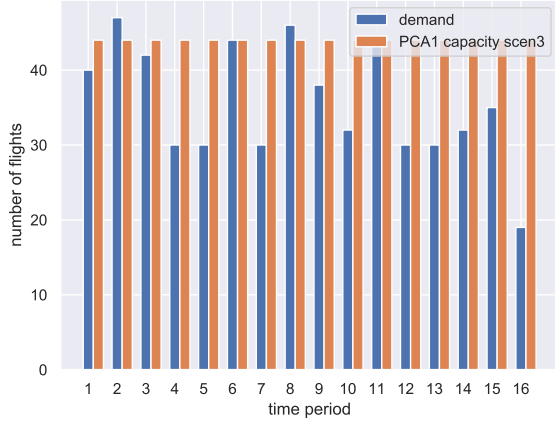


Figure 12: Demand and Capacity at PCA1

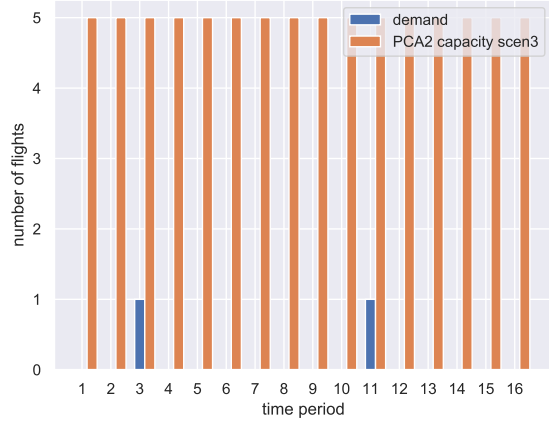


Figure 13: Demand and Capacity at PCA2

- The two-stage solution outperforms the deterministic policy (Scen1-3 and EEV), as it should, since it explicitly considers the uncertainty when making holding decisions. EEV is the expected result of using the EV solution.
- The semi-dynamic model solution is better than the two-stage model solution and dynamic model in turn performs better than semi-dynamic model, which are also expected, because dynamic models uses more weather evolution information than two-stage static model.
- The computation times for all deterministic and stochastic models are all very short. Actually in all cases, integer solution can be obtained from solving the LP relaxation of the problem.

3.8 Formulation Properties

One advantage of aggregate model is that the number of decision variables and constraints do not directly dependent on the number of affected flights. In this use case, the size of static model is relatively small. As model becomes more flexible, the number of variables and constraints increase to the order of tens of thousands.

3.8.1 Totally Unimodularity Properties

Static aggregate multi-commodity CTOP model is the direct generalization of static GDP planning model [33], and the latter has been proved to be Totally Unimodularity (TU) [55][56]. Numerical

Table 3: Aggregate Model Deterministic vs. Stochastic Solutions Comparison

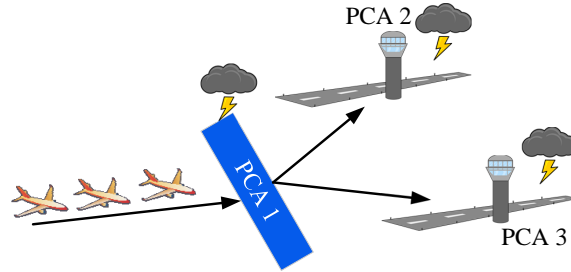
	Ground Delay Periods If This Scenario Occurs:			Air Holding Periods If This Scenario Occurs:			Total Cost If This Scenario Occurs:			Expected Cost	Running Time Seconds
	Scen1	Scen2	Scen3	Scen1	Scen2	Scen3	Scen1	Scen2	Scen3		
Scen1	93	93	93	0	194	391	93	481	875	482.8 (LP Rlx)	$\ll 1.0$
Scen2	284	284	284	0	0	200	284	284	684	404.0 (LP Rlx)	$\ll 1.0$
Scen3	484	484	484	0	0	0	484	484	484	484.0 (LP Rlx)	$\ll 1.0$
EV										166.0 (LP Rlx)	$\ll 1.0$
EEV	166	166	166	0	121	318	166	408	802	453.6 (LP Rlx)	$\ll 1.0$
Two-Stage Model	284	284	284	0	0	200	284	284	684	404.0 (LP Rlx)	0.17
Semi-Dynamic Model	165	284	415	0	0	69	165	284	484	329.0 (LP Rlx)	0.67
Dynamic Model	126	284	479	0	0	9	126	284	488	300.5 (LP Rlx)	1.19
Perfect Information	93	284	484	0	0	0	93	284	484	286.7	

Table 4: Complexity of Aggregate Models

	Variables	Constraints	Non-zeros
Static	1,813	1,924	5,293
Semi-dynamic	14,889	9,141	42,456
Dynamic	22,752	16,274	49,405

results of this use case have shown that LP relaxation solution of static aggregate CTOP model is also integral. In this section, it will be shown that even in deterministic case, aggregate CTOP model is not TU. This is not surprising since it is well known that in general multi-commodity flow is not TU [57].

In the following small example (Figure 14), there are three congested resources, one en route region and two terminal airports. The travel time from the en route region to both airports are equal to one time unit, the planning horizon is 3 time periods, and the capacity information is known perfectly. The coefficient matrix is listed in Table 5. We find a submatrix (35) whose determinant is 2. Thus, in general aggregate CTOP model is NOT TU.

**Figure 14:** Counterexample of TU Property of Aggregate Model

$$\det \begin{pmatrix} -1 & 0 & 0 & 0 & -1 & 0 & 0 & 0 & 0 \\ 1 & 0 & 0 & 0 & 0 & -1 & 0 & 0 & 0 \\ 0 & -1 & 0 & 0 & 0 & 0 & -1 & 0 & 0 \\ 0 & 1 & -1 & 0 & 0 & 0 & 0 & 0 & 0 \\ 0 & 0 & 1 & 0 & 0 & 0 & 0 & -1 & 0 \\ 0 & 0 & 0 & 1 & 0 & 0 & 0 & 0 & -1 \\ 0 & 0 & 0 & 0 & 1 & 0 & 0 & 0 & 1 \\ 0 & 0 & 0 & 1 & 0 & 0 & 1 & 0 & 0 \\ 0 & 0 & 0 & 0 & 0 & 1 & 0 & 1 & 0 \end{pmatrix} = 2 \quad (35)$$

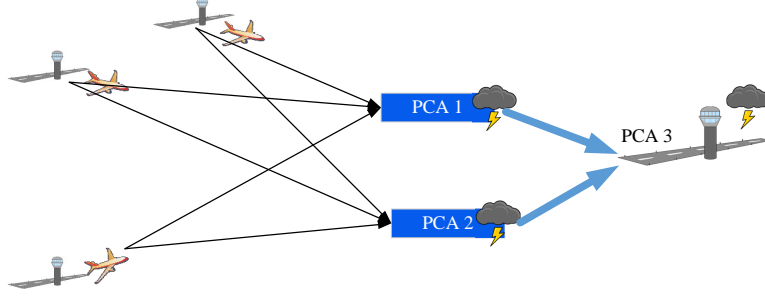


Figure 15: Illustration of Lagrangian-Eulerian Model

It will be shown that Lagrangian part of model is a generalization of Bertsimas and Patterson model [22], the Eulerian part of model is based on the aggregate model proposed in the previous section.

In this section, we will first describe the formulations of two classes of models. For each class, similarly to the last section, there are two-stage static, multistage semi-dynamic and dynamic models. Hence in total there will be 6 stochastic models. Next, we will show how to limit the maximum ground and air delay a flight can take, and how short-term weather forecast and required minimum notification time will affect the nonanticipativity constraints. In section 4.6 and 4.7, we will investigate model formulation properties and numerical results. In section 4.8, we will briefly recapitulate and compare the aggregate and disaggregate models introduced so far. In the end, we will summarize the contributions of this section.

4.2 Two-stage Static Models

In this section, we introduce the Lagrangian and Lagrangian-Eulerian versions of two-stage stochastic model. In two-stage models, the first stage decisions are the reroute decision and ground delay assignment, and the second stage decisions are the air delays flights need to take in response to the actual weather scenarios.

The primary decision variable in this work is w_{ijt}^{rq} , which is a binary variable indicating whether flight i will take j and departs from/passes through airport/PCA r by time t . To be more clear, when r is an airport ($r = \Omega_{ij}^0$), and if route j is chosen for flight i , $w_{ijt}^{rq} = 0$ implies that flight is still on the ground. The first time period $w_{ijt}^{rq} = 1$ is when this flight is released for departure. When r represents a PCA and j is chosen, $w_{ijt}^{rq} = 0$ means flight i is still on its way to PCA r , and w_{ijt}^{rq} first becomes 1 when it is admitted to PCA r . In two-stage stochastic model, the first stage decisions are made while a flight is still on the ground and are the same for all scenarios, hence we can drop superscript q in $w_{ij\bar{T}_{ij}}^r$ when $r = \Omega_{ij}^0$.

4.2.1 Lagrangian Version

In the first set of constraints we ensure that one and only route is chosen for each flight:

$$\begin{aligned} w_{ij\bar{T}_{ij}}^r &= \delta_{ij} & \forall i \in \mathcal{F}, j \in \mathcal{F}_i, r = \Omega_{ij}^0 \\ \sum_{j \in \mathcal{F}_i} \delta_{ij} &= 1 & \forall i \in \mathcal{F} \end{aligned} \tag{36}$$

If j is indeed selected for flight i , then this flight must depart by the last allowed departure time period \bar{T}_{ij}^r . Here δ_{ij} is only an ancillary variable.

There are two types of connectivity constraints in this problem: connectivity in time and connectivity between resources. Connectivity between time ensures that if a flight has been admitted to a

resource by time t , then $w_{ij,t'}^r$ has to be 1 for all later time periods $t' > t$.

$$\begin{aligned} w_{ij,t}^r - w_{ij,t-1}^r &\geq 0 \quad \forall i \in \mathcal{F}, j \in \mathcal{F}_i, r \in \Omega_{ij}^0, t \in T_{ij}^r, q \in Q \\ w_{ij,t}^{r,q} - w_{ij,t-1}^{r,q} &\geq 0 \quad \forall i \in \mathcal{F}, j \in \mathcal{F}_i, r \in \Omega_{ij}^{k \geq 1}, t \in T_{ij}^r, q \in Q \end{aligned} \quad (37)$$

Connectivity constraint between resources imposes that if a flight passes through resource r' by $t + \Delta^{r,r'}$, it must have been admitted to r , which is the upstream resource on route j , by t .

$$\begin{aligned} w_{ij,t+\Delta^{r,r'}}^{r',q} - w_{ij,t}^r &\leq 0 \quad \forall i \in \mathcal{F}, j \in \mathcal{F}_i, r = \Omega_{ij}^0, r' = \Omega_{ij}^1, t \in T_{ij}^r \\ w_{ij,t+\Delta^{r,r'}}^{r',q} - w_{ij,t}^{r,q} &\leq 0 \quad \forall i \in \mathcal{F}, j \in \mathcal{F}_i, r, r' \in \Omega_{ij}^{k \geq 1}, t \in T_{ij}^r \end{aligned} \quad (38)$$

The capacity constraint stipulates that the number of flights admitted to PCA r should not exceed its actual capacity in time period t .

$$\sum_{(i,j) \in \Phi_k; t \in T_{ij}^r} (w_{ij,t}^{r,q} - w_{ij,t-1}^{r,q}) \leq M_{tq}^r \quad \forall r \in \Omega_{ij}^{k \geq 1}, t \in \mathcal{T}, q \in Q \quad (39)$$

The boundary conditions are:

$$w_{ij,\underline{T}_{ij}-1}^r = 0 \quad \forall i \in \mathcal{F}, j \in \mathcal{F}_i, r = \Omega_{ij}^0 \quad (40)$$

$$w_{ij,\underline{T}_{ij}-1}^{r,q} = 0 \quad \forall i \in \mathcal{F}, j \in \mathcal{F}_i, r \in \Omega_{ij}^{k \geq 1}, q \in Q \quad (41)$$

$$w_{ij,\underline{T}_{ij}}^{r,q} = \delta_{ij} \quad \forall i \in \mathcal{F}, j \in \mathcal{F}_i, r = \Omega_{ij}^{N_{ij}}, q \in Q \quad (42)$$

Ground delay for flight i is:

$$g_i = \sum_{j \in \mathcal{F}_i} \left[\sum_{t \in T_{ij}^r; r = \Omega_{ij}^0} t(w_{ij,t}^r - w_{ij,t-1}^r) - \delta_{ij} \text{Dep}_i \right] \quad (43)$$

Air delay for flight i under scenario q is:

$$a_{iq} = \sum_{j \in \mathcal{F}_i} \left[\sum_{t \in T_{ij}^r; r = \Omega_{ij}^{N_{ij}}} \left(t(w_{ij,t}^{r,q} - w_{ij,t-1}^{r,q}) - \delta_{ij} t_{ij}^r \right) \right] - g_{iq} \quad (44)$$

In this work, we assume flight cannot depart before scheduled departure time and cannot speed up, therefore $\text{Dep}_i = \underline{T}_{ij}^{\Omega_{ij}^0}$, $t_{ij}^r = \underline{T}_{ij}^{\Omega_{ij}^r}$.

The objective function minimizes the total reroute, ground delay, and expected air delay costs. Arranging the terms in the following formula

$$\min \sum_{i \in \mathcal{F}} \left(c_g g_i + \sum_{q \in Q} c_a a_{iq} + \sum_{j \in \mathcal{F}_i} c_{ij} \delta_{ij} \right)$$

we obtain

$$\begin{aligned} \min \quad & \sum_{i \in \mathcal{F}} \sum_{j \in \mathcal{F}_i} \left[c_{ij} \delta_{ij} + (c_g - c_a) \sum_{t \in T_{ij}^r; r = \Omega_{ij}^0} \left(t(w_{ij,t}^r - w_{ij,t-1}^r) - \delta_{ij} \underline{T}_{ij}^r \right) + \right. \\ & \left. c_a \sum_{t \in T_{ij}^r; r = \Omega_{ij}^{N_{ij}}} \left(t(w_{ij,t}^{r,q} - w_{ij,t-1}^{r,q}) - \delta_{ij} t_{ij}^r \right) \right] \end{aligned} \quad (45)$$

4.2.2 Lagrangian-Eulerian Version

If we assume the travel time between two consecutive PCAs is the same for all flights, which is a rather mild condition and a common assumption in Eulerian models, we can cluster flights by paths and get a more aggregate Lagrangian-Eulerian formulation.

The Lagrangian-Eulerian formulation is listed below. As mentioned section 4.1, once a flight has chosen a route, left the airport and *arrives at* the first PCA on the picked route, it will be grouped into traffic flows along that path. That is exactly what constraints (53) describes. The key word here is *arrive at*, which is different from *pass through*.

$$\min \sum_{i \in \mathcal{F}} \sum_{j \in \mathcal{F}_i} \left[c_{ij} \delta_{ij} + (c_g - c_a) \sum_{t \in T_{ij}^r; r = \Omega_{ij}^0} \left(t(w_{ij,t}^r - w_{ij,t-1}^r) - \delta_{ij} T_{ij}^r \right) \right] + c_a \sum_{q \in Q} p_q \sum_{t \in T} \sum_{\rho \in \mathcal{P}} \sum_{k \in \rho} A_{t,\rho}^{k,q} \quad (46)$$

$$w_{ij,T_{ij}^r}^r = \delta_{ij} \quad \forall i \in \mathcal{F}, j \in \mathcal{F}_i, r = \Omega_{ij}^0 \quad (47)$$

$$\sum_{j \in \mathcal{F}_i} \delta_{ij} = 1 \quad \forall i \in \mathcal{F} \quad (48)$$

$$w_{ij,t}^r - w_{ij,t-1}^r \geq 0 \quad \forall i \in \mathcal{F}, j \in \mathcal{F}_i, r = \Omega_{ij}^0, t \in T_{ij}^r, q \in Q \quad (49)$$

$$\tilde{w}_{ij,t}^{r',q} - \tilde{w}_{ij,t-1}^{r',q} \geq 0 \quad \forall i \in \mathcal{F}, j \in \mathcal{F}_i, r' = \Omega_{ij}^1, t \in T_{ij}^{r'}, q \in Q \quad (50)$$

$$w_{ij,T_{ij}^r-1}^{r,q} = \tilde{w}_{ij,T_{ij}^{r'}-1}^{r',q} = 0 \quad \forall i \in \mathcal{F}, j \in \mathcal{F}_i, r = \Omega_{ij}^0, r' = \Omega_{ij}^1, q \in Q \quad (51)$$

$$\tilde{w}_{ij,t+\Delta^{r,r'}}^{r',q} - w_{ij,t}^r = 0 \quad \forall i \in \mathcal{F}, j \in \mathcal{F}_i, r = \Omega_{ij}^0, r' = \Omega_{ij}^1, t \in T_{ij}^r \quad (52)$$

$$P_{t,\rho}^k = \sum_{(i,j) \in \Phi_k; j \in \rho} \sum_{t \in T_{ij}^r; r = \Omega_{ij}^1} (\tilde{w}_{ij,t}^r - \tilde{w}_{ij,t-1}^r) \quad \forall t \in T, \rho \in \mathcal{P}, k = \rho_1 \quad (53)$$

$$L_{t,\rho}^{k,q} = \begin{cases} \text{if } k = \rho_1 & P_{t,\rho}^k - (A_{t,\rho,q}^k - A_{t-1,\rho,q}^k) \\ \text{else} & \text{UpPCA}_{t,\rho,q}^k - (A_{t,\rho,q}^k - A_{t-1,\rho,q}^k) \end{cases} \quad \forall t \in T, q \in Q, \rho \in \mathcal{P}, k \in \rho \quad (54)$$

$$\text{UpPCA}_{t,\rho,q}^k = L_{t-\Delta^{k',k},\rho}^{k',q} \quad t \in T, q \in Q, (k', k) \in \rho \quad (55)$$

$$\sum_{t \in T} P_{t,\rho}^{k=\rho_1} = \sum_{t \in T} L_{t,\rho}^{k=\rho-1,q} \quad \forall \rho \in \mathcal{P}, q \in Q \quad (56)$$

$$P_{t,\rho}^k, L_{t,\rho}^{k,q}, A_{t,\rho,q}^k \geq 0 \quad \forall t \in T, q \in Q, \rho \in \mathcal{P}, k \in \rho \quad (57)$$

$$\sum_{\rho \in \mathcal{P}} L_{t,\rho}^{k,q} \leq M_{t,q}^k \quad \forall t \in T, q \in Q, k \in \mathcal{P} \quad (58)$$

4.3 Multistage Dynamic Models

In this section, we introduce the multistage stochastic models which can dynamically adjust flight release time and reroute choice before actual departure.

4.3.1 Lagrangian Version

The formulation is listed as follows:

$$\min \sum_{q \in Q} p_q \sum_{i \in \mathcal{F}} \sum_{j \in \mathcal{F}_i} \left[\left(c_{ij} - (c_g - c_a) T_{ij}^{r=\Omega_{ij}^0} - c_a T_{ij}^{r=\Omega_{ij}^{N_{ij}}} \right) \tilde{\delta}_{qij} + (c_g - c_a) \sum_{t \in T_{ij}^r; r = \Omega_{ij}^0} t(w_{ij,t}^{r,q} - w_{ij,t-1}^{r,q}) + c_a \sum_{t \in T_{ij}^r; r = \Omega_{ij}^{N_{ij}}} t(w_{ij,t}^{r,q} - w_{ij,t-1}^{r,q}) \right] \quad (59)$$

$$\delta_{qtij} = w_{ijt}^{r,q} - w_{ij,t-1}^{r,q} \quad \forall i \in \mathcal{F}, j \in \mathcal{F}_i, r = \Omega_{ij}^0, q \in Q \quad (60)$$

$$\tilde{\delta}_{qij} = \sum_{t \in T_{ij}^r; r = \Omega_{ij}^0} \delta_{qtij} \quad \forall i \in \mathcal{F}, j \in \mathcal{F}_i, q \in Q \quad (61)$$

$$\sum_{j \in \mathcal{F}_i} \tilde{\delta}_{qij} = 1 \quad \forall i \in \mathcal{F}, q \in Q \quad (62)$$

$$w_{ij,t}^{r,q} - w_{ij,t-1}^{r,q} \geq 0 \quad \forall i \in \mathcal{F}, j \in \mathcal{F}_i, r \in \Omega_{ij}, t \in T_{ij}^r, q \in Q \quad (63)$$

$$w_{ij,t+\Delta r,r'}^{r',q} - w_{ij,t}^{r,q} \leq 0 \quad \forall i \in \mathcal{F}, j \in \mathcal{F}_i, r, r' \in \Omega_{ij}, t \in T_{ij}^r \quad (64)$$

$$\sum_{(i,j) \in \Phi_k; t \in T_{ij}^r} (w_{ijt}^{r,q} - w_{ij,t-1}^{r,q}) \leq M_{tq}^r \quad \forall r \in \Omega_{ij}^{k \geq 1}, t \in \mathcal{T}, q \in Q \quad (65)$$

$$\delta_{q_1^b tij} = \dots = \delta_{q_{N_b}^b tij} \quad \forall i \in \mathcal{F}, j \in \mathcal{F}_i, t \in T_{ij}^{\Omega_{ij}^0}, b \in B, \mu_b \geq t \geq o_b \quad (66)$$

$$w_{ij, \underline{T}_{ij}^r - 1}^{r,q} = 0 \quad \forall i \in \mathcal{F}, j \in \mathcal{F}_i, r \in \Omega_{ij}, q \in Q \quad (67)$$

$$w_{ij, \underline{T}_{ij}^r}^{r,q} = \tilde{\delta}_{qij} \quad \forall i \in \mathcal{F}, j \in \mathcal{F}_i, q \in Q, r = \Omega_{ij}^{N_{ij}} \quad (68)$$

The first three sets of constraints make sure one and only route will be chosen for each flight. δ_{qtij} is an ancillary binary variable indicating whether flight will take route j and depart in time period t . $\tilde{\delta}_{qij}$ is another ancillary variable which shows whether flight will choose route j under scenario q . (63) and (64) are connectivity in time constraint and connectivity between resources constraint. (65) is the capacity constraint, which has exactly the same expression as in the two-stage model. In multistage model, we will also have a set of nonanticipativity constraints (66), which ensures that decisions are made solely based on the information available at that time. (67) and (68) are boundary conditions.

4.3.2 Lagrangian-Eulerian Version

The dynamic Lagrangian-Eulerian model is straightforward. The ‘‘Lagrangian part’’ is similar to several constraints in dynamic Lagrangian model, and the ‘‘Eulerian part’’ is the exactly same as in the static Lagrangian-Eulerian except for the additional superscript q in $P_{t,\rho}^{k,q}$ and $\tilde{w}_{ij,t}^{r',q}$.

$$\min \sum_{q \in Q} p_q \left[\sum_{i \in \mathcal{F}} \sum_{j \in \mathcal{F}_i} \sum_{t \in T_{ij}^r; r = \Omega_{ij}^0} (c_g(t - \underline{T}_{ij}^{r = \Omega_{ij}^0}) + c_{ij}) \delta_{qtij} + c_a \sum_{t \in T} \sum_{\rho \in \mathcal{P}} \sum_{k \in \rho} A_{t,\rho}^{k,q} \right] \quad (69)$$

$$\delta_{qtij} = w_{ijt}^{r,q} - w_{ij,t-1}^{r,q} \quad \forall i \in \mathcal{F}, j \in \mathcal{F}_i, r = \Omega_{ij}^0, q \in Q \quad (70)$$

$$\tilde{\delta}_{qij} = \sum_{t \in T_{ij}^r; r = \Omega_{ij}^0} \delta_{qtij} \quad \forall i \in \mathcal{F}, j \in \mathcal{F}_i, q \in Q \quad (71)$$

$$\sum_{j \in \mathcal{F}_i} \tilde{\delta}_{qij} = 1 \quad \forall i \in \mathcal{F}, q \in Q \quad (72)$$

$$w_{ij,t}^{r,q} - w_{ij,t-1}^{r,q} \geq 0 \quad \forall i \in \mathcal{F}, j \in \mathcal{F}_i, r = \Omega_{ij}^0, t \in T_{ij}^r, q \in Q \quad (73)$$

$$\tilde{w}_{ij,t}^{r',q} - \tilde{w}_{ij,t-1}^{r',q} \geq 0 \quad \forall i \in \mathcal{F}, j \in \mathcal{F}_i, r' = \Omega_{ij}^1, t \in T_{ij}^{r'}, q \in Q \quad (74)$$

$$\tilde{w}_{ij,t+\Delta r,r'}^{r',q} - \tilde{w}_{ij,t}^{r,q} = 0 \quad \forall i \in \mathcal{F}, j \in \mathcal{F}_i, r = \Omega_{ij}^0, r' = \Omega_{ij}^1, t \in T_{ij}^r \quad (75)$$

$$\delta_{q_1^b tij} = \dots = \delta_{q_{N_b}^b tij} \quad \forall i \in \mathcal{F}, j \in \mathcal{F}_i, t \in T_{ij}^{\Omega_{ij}^0}, b \in B, \mu_b \geq t \geq o_b \quad (76)$$

$$w_{ij, \underline{T}_{ij}^r - 1}^{r,q} = \tilde{w}_{ij, \underline{T}_{ij}^r - 1}^{r',q} = 0 \quad \forall i \in \mathcal{F}, j \in \mathcal{F}_i, r = \Omega_{ij}^0, r' = \Omega_{ij}^1, q \in Q \quad (77)$$

$$\tilde{w}_{ij, \bar{T}_{ij}^{r'}}^{r', q} = \tilde{\delta}_{qij} \quad \forall i \in \mathcal{F}, j \in \mathcal{F}_i, q \in Q, r' = \Omega_{ij}^1 \quad (78)$$

$$P_{t, \rho}^{k, q} = \sum_{(i, j) \in \Phi_k; j \in \rho} \sum_{t \in T_{ij}^r; r' = \Omega_{ij}^1} (\tilde{w}_{ij, t}^{r', q} - \tilde{w}_{ij, t-1}^{r', q}) \quad \forall t \in T, \rho \in \mathcal{P}, k = \rho_1, q \in Q \quad (79)$$

(54) – (58)

4.4 Multistage Semi-dynamic Models

In multistage dynamic models, a flight can revise the departure time and reroute choice multiple times as long as it is on the ground. An important and practical variant of multistage model is semi-dynamic model, in which the ground delay and reroute decisions are made at some pre-determined time, e.g. 1 hour before schedule departure time. For simplicity, we usually assume the decisions are made at the scheduled departure time. Instead of enforcing (66), we will impose the following nonanticipativity constraints in Lagrangian and Lagrangian-Eulerian models:

$$\delta_{q_1^{b_{t_{ij}}} t_{ij}} = \dots = \delta_{q_{N_b}^{b_{t_{ij}}} t_{ij}} \quad \forall i \in \mathcal{F}, j \in \mathcal{F}_i, t \in T_{ij}^{\Omega_{ij}^0}, b \in B, \mu_b \geq \text{Dep}_i \geq o_b \quad (80)$$

The major advantage of semi-dynamic model over dynamic model is the higher predictability in flight schedule.

4.5 Additional Modeling Considerations

4.5.1 Limiting the Amount of Delay

The parameter T directly controls the maximum delay flight i is allowed to take. By setting $\bar{T}_{ij}^{r = \Omega_{ij}^0}$ as a small number, we can limit the amount of allowed ground delay. When two PCAs are very close to each other, it is not realistic for a flight to take even one unit of air delay. In that case, for such (r, r') on route j we can impose that

$$w_{ij, t + \Delta^{r, r'}}^{r'q} - w_{ij, t}^{r'q} = 0 \quad t \in T_{ij}^r \quad (81)$$

In general, if the maximum air delay between (r, r') on route j is $d_{ij}^{r, r'}$, we can add the following set of constraints:

$$w_{ij, t + \Delta^{r, r'} + d_{ij}^{r, r'}}^{r'q} - w_{ij, t}^{r'q} \geq 0 \quad t \in T_{ij}^r \quad (82)$$

which enforces that if a flight has traverses resource r by t , it will reach r' , which is the downstream resource on route j , by $t + \Delta^{r, r'} + d_{ij}^{r, r'}$.

4.5.2 Impact of Short-term Weather Forecast

In the original formulation, it is assumed that scenario tree (Figure 16b) is obtained from probabilistic weather forecast, and the new operational conditions are not known until they have actually changed. In other words, we have to wait until the branch point to know which scenario actually materializes. In reality, since the short-term weather forecast is rather accurate, it is reasonable to assume that we know which scenario will happen a few time periods in advance.

Assuming that the one-hour weather forecast is exactly accurate, then the scenario tree about the weather information (Figure 16a) is the left translation of the scenario tree for actual physical capacity (Figure 16b). For example, at 2000Z or t_1 , which is the beginning of stage 1, we only need to impose

$$\delta_{2, t_1, ij} = \delta_{3, t_1, ij} \quad \forall i \in \mathcal{F}, j \in \mathcal{F}_i, t_1 \in T_{ij}^{\Omega_{ij}^0} \quad (83)$$

even though physical capacities still satisfy $M_{t_1, 1}^r = M_{t_1, 2}^r = M_{t_1, 3}^r$. Compared with the original implementation, because of additional information brought by the short-term weather forecast, the nonanticipativity constraints will be less restrictive and lower system costs can be achieved.

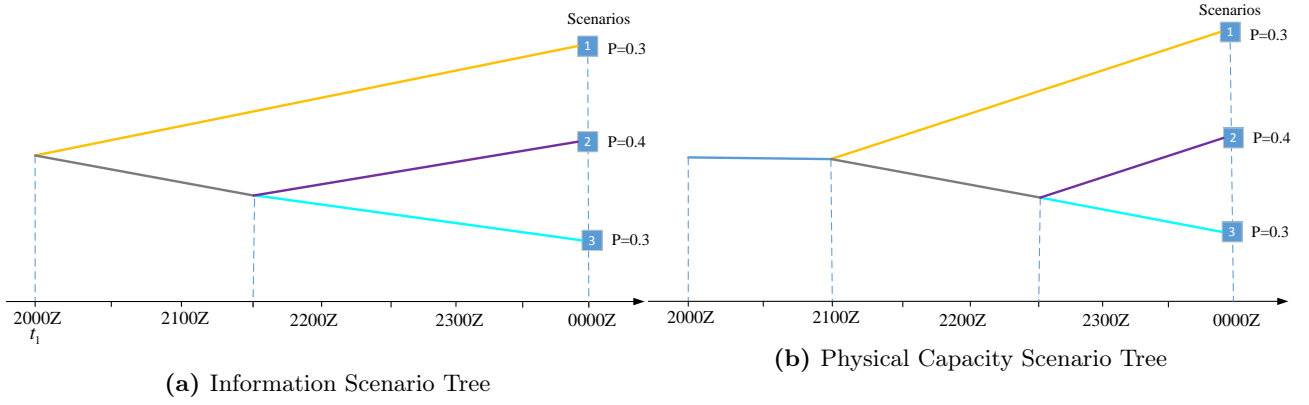


Figure 16: Effect of Short-term Weather Forecast

4.5.3 Impact of Minimum Notification Time

In the original formulation, it is assumed that a flight is ready to take off anytime at or after the scheduled takeoff time. It is more reasonable to require the model to make the ground delay and reroute decision a certain time before the scheduled departure time so that the airline agents can have some preparation time and have time decide when to let passengers board.

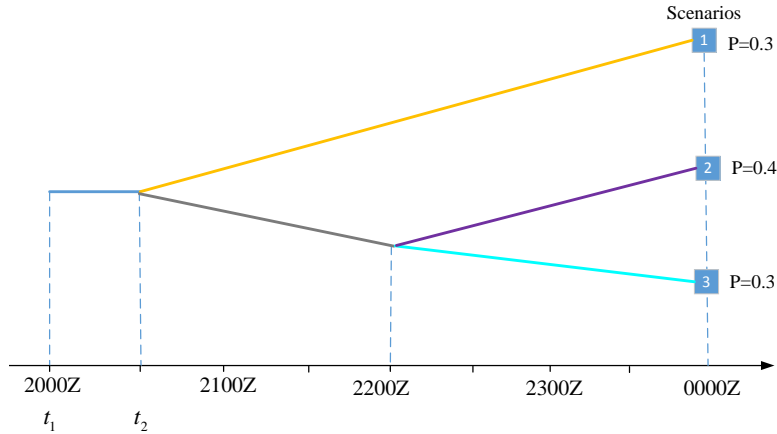


Figure 17: Combined Effect of Short-term Weather Forecast and Minimum Notification Time

For example, if we require the reroute decision to be made 30 minutes before scheduled departure time, the effect is that scenario tree in Figure 16a will be translated 2 time periods to the right, shown in Figure 17. Nonanticipativity constraints need to be modified accordingly.

4.6 Formulation Properties

Before coming up with the formulations introduced in this section, in [58], we proposed an alternative integer programming formulation to solve problem 2. The advantage of this alternative formulation is that ground and air delay are explicit decision variables and are more straightforward to management. For example, it is easier to model flight which speeds up and arrives earlier when flying from one region to another. Since the primary decision variables in the current formulation are all binary, we call the current formulation binary model. The alternative formulation is referred as integer model. In this and next section, we will compare the problem size and computational performance of these two formulations.

Table 6: Model Complexity of Disaggregate Models

			Lagrangian			Lagrangian-Eulerian		
			Variables	Constraints	Non-zeros	Variables	Constraints	Non-zeros
Integer Model	Without TOS	Static	53,462	8,730	152,232	17,532	3,698	51,524
		Semi-dynamic	55,242	9,933	154,638	49,656	8,796	145,902
		Dynamic	97,584	20,892	260,358	91,998	19,758	247,668
	With TOS	Static	63,801	14,969	188,688	27,049	5,144	77,605
		Semi-dynamic	69,273	20,389	204,176	78,087	19,534	237,287
		Dynamic	130,074	30,463	410,111	137,703	25,504	37,2563
Binary Model	Without TOS	Static	65,652	118,368	323,674	33,426	50,490	130,104
		Semi-dynamic	142,452	217,763	565,696	142,350	215,579	559,966
		Dynamic	142,452	204,660	539,490	142,350	202,476	533,760
	With TOS	Static	100,899	181,736	499,104	51,025	77,550	198,859
		Semi-dynamic	219,411	335,868	935,352	217,839	330,672	920,433
		Dynamic	219,411	315,754	895,118	217,839	310,546	880,181

4.7 Model Comparisons

Table 7: Disaggregate Stochastic Models Comparison Without TOS

Lagrangian vs. Lagrangian- Eulerian	Ground Delay Periods			Air Holding Periods			Expected Cost	Integer Model		Binary Model
	If This Scenario Occurs:			If This Scenario Occurs:				Running Time mins	Early Stop at 1min/3mins	Running Time mins
	Scen1	Scen2	Scen3	Scen1	Scen2	Scen3				
Scen1	90	90	90	0	203	411	499.0	< 0.01 (LP Rlx)		< 0.01 (LP Rlx)
Scen2	285	285	285	0	0	218	415.8	< 0.01 (LP Rlx)		< 0.01 (LP Rlx)
Scen3	489	489	489	0	0	0	489.0	< 0.01 (LP Rlx)		< 0.01 (LP Rlx)
Two-stage Model	284	284	284	0	1	205	407.8	0.61		0.12 (LP Rlx)
Semi-dynamic Model	164	285	417	0	0	73	332.1	3.85	334.6/332.1	0.23 (LP Rlx)
Dynamic Model	125	288	477	0	0	13	303.6	> 10.0	306.1/303.9	0.21 (LP Rlx)
Perfect Information	90	285	489	0	0	0	287.7			
Scen1	93	93	93	0	194	391	482.8	< 0.01 (LP Rlx)		< 0.01 (LP Rlx)
Scen2	284	284	284	0	0	200	404.0	< 0.01 (LP Rlx)		< 0.01 (LP Rlx)
Scen3	484	484	484	0	0	0	484.0	< 0.01 (LP Rlx)		< 0.01 (LP Rlx)
Two-stage Model	284	284	284	0	0	200	404.0	0.01 (LP Rlx)		0.04 (LP Rlx)
Semi-dynamic Model	163	284	417	0	0	69	329.0	0.40		0.20 (LP Rlx)
Dynamic Model	127	284	472	0	0	12	300.5	7.69	300.5	0.21 (LP Rlx)
Perfect Information	93	284	484	0	0	0	286.7			

Table 8: Disaggregate Stochastic Models Comparison With TOS

Lagrangian vs. Lagrangian- Eulerian	RTC Costs in Mins			Ground Delay Periods			Air Holding Periods			Expected Cost	Integer Model		Binary Model
	If This Scenario Occurs:			If This Scenario Occurs:			If This Scenario Occurs:				Running Time mins	Early Stop at 1min/3mins	Running Time mins
	Scen1	Scen2	Scen3	Scen1	Scen2	Scen3	Scen1	Scen2	Scen3				
Scen1	76	76	76	56	56	56	0	142	285	350.73	< 0.01 (LP Rlx)		< 0.01 (LP Rlx)
Scen2	222	222	222	109	109	109	0	0	70	180.60	< 0.01 (LP Rlx)		< 0.01 (LP Rlx)
Scen3	286	286	286	144	144	144	0	0	0	182.13	< 0.01 (LP Rlx)		< 0.01 (LP Rlx)
Two-stage Model	272	272	272	108	108	108	0	0	38	167.07	0.20		0.19 (LP Rlx)
Semi-dynamic Model	216	256	268	86	108	130	0	0	22	154.21	0.08		0.64 (LP Rlx)
Dynamic Model	216	256	268	73	110	136	0	0	16	149.31	1.86	149.31	0.58 (LP Rlx)
Perfect Information	76	222	286	56	109	144	0	0	0	129.92			
Scen1	76	76	76	58	58	58	0	141	308	365.73	< 0.01 (LP Rlx)		< 0.01 (LP Rlx)
Scen2	222	222	222	105	105	105	0	0	69	176.00	< 0.01 (LP Rlx)		< 0.01 (LP Rlx)
Scen3	286	286	286	132	132	132	0	0	0	170.13	< 0.01 (LP Rlx)		< 0.01 (LP Rlx)
Two-stage Model	270	270	270	106	106	106	0	0	29	159.40	< 0.01		0.02 (LP Rlx)
Semi-dynamic Model	216	256	268	84	104	123	0	1	26	147.11	0.09		0.09 (LP Rlx)
Dynamic Model	216	256	268	74	105	128	0	0	13	143.41	0.49		0.13 (LP Rlx)
Perfect Information	76	222	286	58	105	132	0	0	0	125.32			

The main results are listed in Tables 7 and 8. There are some key findings from the tables:

1. The first row of Table 7 should be read as follows: if we plan ground delay only according to

scenario 1 and ignore the information of scenario 2 and 3, the deterministic policy obtained tells us that a total of 90 units of ground delay need to be assigned to flights. If we implement this deterministic policy in reality, the expected cost under all scenarios is 499.0.

Note that when planning ground delay it is possible there are two deterministic policies which achieve the same objective value. But when implementing these two policies, one obtains lower expected cost than other one.

2. There are small discrepancies between Lagrangian and Lagrangian-Eulerian model results. For example, the objective value of two-stage with TOS Lagrangian model is 407.8, whereas the corresponding Lagrangian-Eulerian model value is 404.0. The cause of this difference is that the travel time between two PCAs may differ for different flights. In Lagrangian-Eulerian model, average travel time is used when planning the traffic flows.
3. Lagrangian-Eulerian models without TOS also solve the problem 1. If we compare the solutions with aggregate model results in Table , they are exactly the same, which is anticipated.
4. The overall system cost could decrease by over 50% if flight operators submit TOS options for flights. This shows the huge benefit of allowing rerouting in the face of congestion.
5. The two-stage solution outperforms the deterministic policy (Scen 1-3), as it should, since it explicitly considers the uncertainty when making holding decisions. The semi-dynamic model solution is better than the two-stage model solution, and the dynamic model in turn performs better than the semi-dynamic model, which is also expected, because the dynamic model uses more weather evolution and flight schedule information than the two-stage static model.
6. In the case where flights do not have reroute options, adjusting ground-holding policy is vital and brings down the cost by over 25%. If flights can choose to reroute, the benefit of dynamically changing departure time is less significant, but can still decrease the total cost by more than 10% if using a fully dynamic case instead of a deterministic or a two-stage stochastic model.
7. In this use case, integer solutions can be directly obtained from linear programming relaxation, for all six stochastic binary models and for both no-route and reroute cases. Whereas in previous integer formulation, we had fractional solutions from solving linear relaxation. This indicates that binary model formulation seems to be a stronger formulation compared with previous integer formulation.
8. Lagrangian-Eulerian models are in general considerably faster than Lagrangian models. This is one of the motivations to develop Lagrangian-Eulerian models.

4.8 Summary of Aggregate and Disaggregate Models

In this section, we summarize and compare 9 CTOP related stochastic models we have introduced so far, which are listed in Table 9. This table not only elucidates the nuances of different CTOP models, but also can guide researchers to develop new models for future TMIs, which is valuable for air traffic flow management research.

Table 9: Comparison of Aggregate and Disaggregate Stochastic CTOP Models

	Aggregate models	Disaggregate models	Disaggregate-aggregate models
	Eulerian models	Lagrangian models	Lagrangian-Eulerian models
Static	[59] §IV	[58] §IIIA	[58] §IIIB
Semi-dynamic	[59] §V	[58] §IVA	[58] §IVB
Dynamic	[59] §VI	[58] §VA	[58] §VB

It is not hard to see that none of these 9 models can be directly used in the current CTOP software. Aggregate models are proposed to solve problem 1, which do not consider demand uncertainty. Two classes of disaggregate models are formulated to tackle problem 2, which are based on the assumption that ground delay and reroute can be directly assigned by FAA traffic managers. In addition, all semi-dynamic and dynamic models are not compatible with the current CDM-CTOP software because current software does not support conditional delay (and reroute) decisions, same as in the GDP case.

In the literature, one definition of CDM-compatibility is that the model should be able to accommodate FAA and airline operations, including intra-airline cancellation and substitution and slot compression, etc. In this loose sense, the disaggregate models can be made to be consistent with CDM philosophy, as introduced in [60].

Aggregate models can be seen as solutions to an intermediate TMI between GDP/AFP and CTOP. Moreover, once flights have chosen route, aggregate model can be used as basis for traffic flow simulation, as will be discussed in section A.5.

4.9 Conclusions

In this section, six stochastic models are proposed to address problem 2 (section 1.3), which generalize the classical GDP planning models to the case of multiple constrained regions multiple reroute options. Similar to the last section, we have demonstrated the benefits of making use of scenario tree, flight information and developing dynamic stochastic models. We have shown how additional short-term weather information and additional minimum notification time requirement can affect the implementation of nonanticipativity constraints, and how we can incorporate variance and risk considerations and still have MILP formulation. Though important information can be obtained from solving aggregate and disaggregate models, we point out that they do not address problem 3, which will be solved in section 5.

5 Stochastic and Simulation-based Optimization Model for Setting Flow Rates in Collaborative Trajectory Options Program

5.1 Introduction

In this section, we address the problem 3 in section 1.3. It is fair to say that problem 1 and 2 play important ancillary roles in this work, while problem 3 is the very problem we want to solve because it is the exact real-world problem that has practical value.

In aggregate and disaggregate models, the concept of FCA is not used, whereas the goal in problem 3 is to set traffic flow rates for FCAs in CTOP. In section 5.2, we discuss in detail about the differences between FCA and PCA, properties of FCA-PCA network, etc. There are two natural ideas to handle TOS-induced demand uncertainty in CTOP:

1. Design algorithm that only uses capacity information to decide FCA rates.
2. Start with a demand estimation, iteratively compute the traffic flow rate, then re-estimate the demand. Hopefully after each iteration demand estimation can be improved, and after a few iterations, the computation loop will converge and optimal traffic flow rates can be obtained.

For the first thought, it has been proved in [64] that even in this single congested region case, in general this kind of algorithm cannot provide optimal solution. For the second thought, a computation loop will be needed. In section 5.3, we will explain why this computation loop will converge to bad solution due to conservative planned acceptance rates issue explained in [64], and the demand shift issue. In section 5.4, we will talk about how simulation-based optimization can bypass these two issues and provide good suboptimal solution. Saturation technique and these two natural ideas will only be used as heuristics to compute initial search points. Then local search algorithm will be applied to find better candidate solutions. Numerical results will be introduced in section 5.4.2. In section 5.5, we will recapitulate the findings in this section.

5.2 Flow Constrained Area, Ground Delay and Traffic Flow Rates

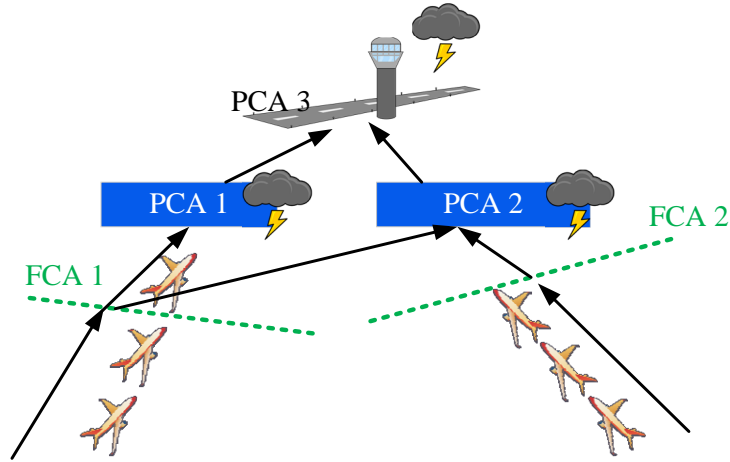


Figure 18: Illustration of FCAs and PCAs

5.2.1 Flow Constrained Area and Potentially Constrained Area

As mentioned in section 2.1.2, Flow Constrained Area (FCA) was first introduced in AFP to model en route airspace constraint. Different from a PCA which coincides with a physically constrained area and whose future capacity is stochastic, a FCA is an artificial line or region in the airspace and serves like a valve to control traffic flows into a region. In this work, The future capacity of a PCA is modeled as scenario-based, which corresponds to multiple sets of possible capacity values, e.g. PCA0 in Table 2. By contrast, planned acceptance rates of a FCA correspond to a single vector. Figure 18 depicts both FCAs and PCAs in a traffic management setting.

In AFP, the distinction between FCA and PCA was not made in the literature, because there is one constrained region (PCA), and the FCA can be considered as directly lying atop that PCA. In CTOP, we need to explicitly distinguish the control mechanism (FCA) with the source of congestions (PCA) for two major reasons. First, the number of FCAs may not be the same as the number of PCAs, and FCAs may not co-locate with PCAs. Second, a FCA corresponds to ground delay at departure airports, whereas traversing a PCA corresponds to scenario-dependent air delay. Since it does not make sense for a flight to take scenario-dependent air delay after pass a PCA, then take ground delay at its origin airport, therefore traffic flows from PCAs can not be fed into FCAs, consequently FCAs and PCAs need to be differentiated.

5.2.2 FCA-PCA Network, Why One FCA for Each Path

In the section, the concept of FCA-PCA network is used, which is a directed graph that links FCAs and PCAs and is an extension to the PCA network. This concept gives structure to our problem and allows us to use various network flow optimization techniques.

5.2.3 Implicit FCAs in Aggregate Models, Scenario-dependent Ground Delay

A FCA controls the traffic flow by assigning slots to its impacted flights, which can be translated into ground delays. In static aggregate model, flights are assigned with ground delays before entering into PCAs. Essentially, it can be understood that *for each path* there is an implicit FCA lies atop of the first PCA of that path. In semi-dynamic and dynamic aggregate models, flights are assigned with scenario-dependent ground delays. Since the current definition of FCA does not support scenario-dependent conditional slots, therefore FCA cannot be used in semi-dynamic and dynamic models.

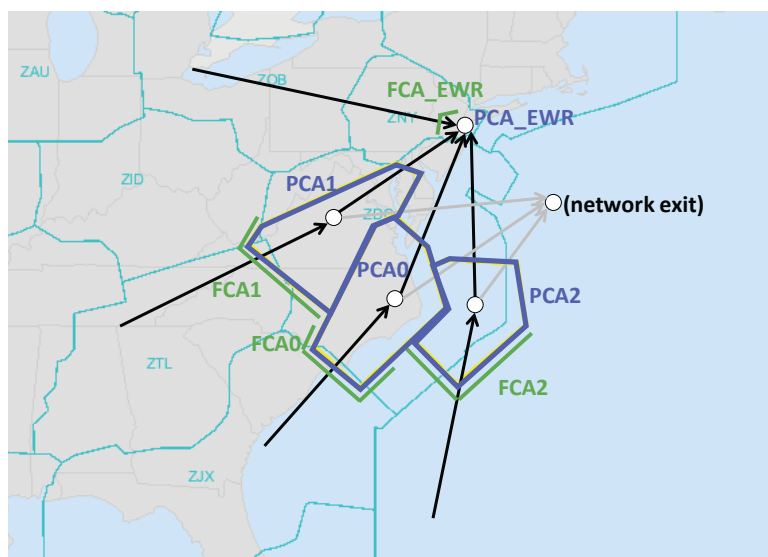


Figure 19: Geographical Display of the FCA-PCA Network

From the above discussion we can see that FCA is only an artificial concept, and in some cases it is not needed in mathematical formulation and in managing traffic flows.

5.2.4 Implication of One FCA Managing Multiple “Paths” of Traffic Flows

In Figure 19, air traffic managers create one FCA for each PCA, which is in line with the intuition. In this case, for example, FCA1 will control flights on two paths. However, in general, using one FCA to manage multiple traffic streams is not the optimal way to manage the traffic flow.

Assume the route information of each flight is known (the same assumption we made for aggregate models), there are two ways to optimize FCA planned acceptance rates:

1. In the direct way, we need to model the split of traffic flow out of FCA1. To make sure the model is linear, the flow split ratios need to be pre-calculated as parameters. Since they are calculated using schedule data, if some flights are ground delayed for one time period, then the model will use flow split ratio in the next time period to model the movement of these flights, which will likely result in the violation the original flight route schedules. Also, since these ratios are real numbers, we cannot impose integrality constraints on decision variables. Hence, optimal solution is not guaranteed.
2. In the indirect way, we can run static aggregate model and obtain the planned acceptance rates for path PCA1→ EWR and path PCA1→ exit, then sum these two rates to get the rates for FCA1. This is only a heuristic and there is no optimality guarantee.

The conclusion is that, assume demand is known, to manage multiple constrained resources precisely and optimally, we need one FCA for each path of flights. And FCA designed for controlling flights on one path needs to exempt flights belonging to other paths.

5.3 CTOP FCA Rates Planning, Demand Shift Issue, Rate Computation Loop

In this section, we first explain why CTOP FCA rates planning problem cannot be solved as a single MILP model like in the disaggregate model or in the GDP planned problem. Next, we introduce the idea of rate computation loop. Then we talk about why this seemingly attractive idea, if not using with additional heuristics, will result in bad solution. This section shows the complexity of solving problem 3 only in the stochastic programming framework, and motivates us to tackle this problem using simulation-based optimization approach.

5.3.1 Why Not Single Optimization Model, Rate Computation Loop

The main reason why a single MILP model is not sufficient to address problem 3 is that we need to follow CDM principle. Ground delay and route assignments have to comply with CTOP slot allocation algorithm, which is highly nonlinear (appendix). Optimizing reroute and delay for each flight while ignoring slot allocation rules is relative easy, as we have done in section 4. However, it is intractable to optimize reroute and delay at the same time while exactly satisfying all the rules in the slot allocation algorithm.

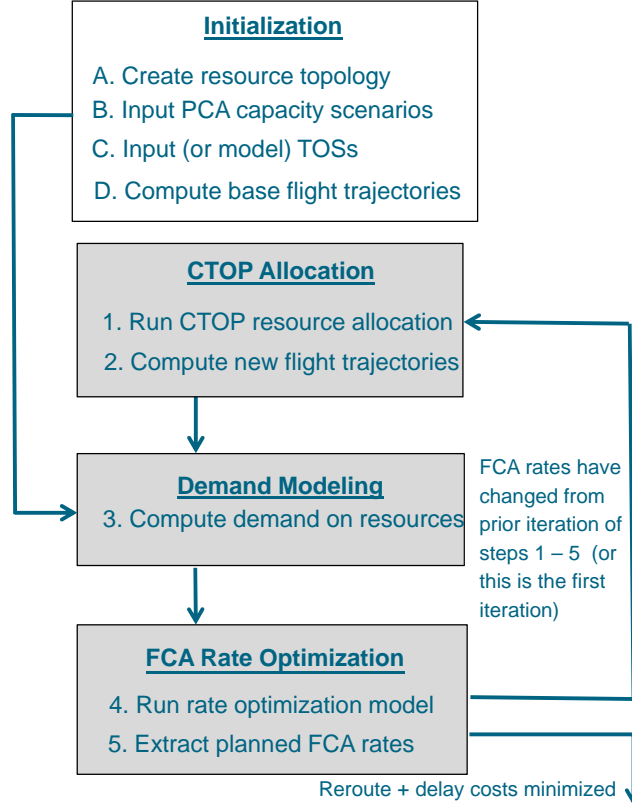


Figure 20: Rate Computation Loop

As proved in [64], in general demand information is needed to make optimal traffic flow rates decision. In CTOP, due to TOS-induced demand uncertainty, demand information is unknown to air traffic managers before setting the FCA rates. To solve this dilemma, an idea is to start with a demand estimation, e.g. assuming all flights will choose their most preferred routes, then solve FCA rates planning problem with know demand, which is an easy problem and almost the same problem has been addressed by static aggregate model. This computation loop is shown in Figure 20. After getting FCA rates, we run the TOS allocation algorithm, which ensures fairness in this iteration, get the new route and ground delay for each flight, and compute the new demand to each congested region. It is hoped that compared with the initial demand estimation, this will be a better estimation. Based on this new demand estimation, we will do another iteration of FCA rates optimization. Clearly, there is a computation loop here. We name it Rate Computation Loop [65].

Ideally, rate computation loop will converge after few iterations and will converge to good FCA rates solution. In practice, there is no need to worry about the convergence issue. We only need to run it for several iterations and pick the FCA rates that minimize total reroute and delay costs.

In the next section, we will explain why the intuition about rate computation loop is wrong, if no additional heuristics are used.

5.3.2 Demand Shift Issue and Conservative FCA Rates Issue

Demand shift issue in CTOP refers to the phenomenon that after solving the rate planning optimization problem given a demand estimation and run CTOP slot allocation algorithm, the demand may shift from one FCA to another FCA, and invalidate the proposed acceptance rates. In rate computation loop, it is addressed by resolving rates optimization problem whenever demand changes.

Conservative FCA rates issue, which was introduced in [64], refers to the fact that in air traffic flow rate optimization models, the planned traffic rates are computed based on the lesser of demand and capacity. We have shown that this issue makes static GDP model susceptible to demand uncertainty. However, if this is considered a minor defect for GDP problem, then it is a major problem in CTOP FCA rates planning. If in the first iteration, very few or no flights are scheduled to traverse a certain FCA, then FCA rates computed from rate optimization model would be near or equal to zero. The CTOP allocation algorithm will consider this FCA being heavily restricted/fully blocked and will allocate very few/no slots to flights. Then in the next iteration, there will be very few/no flights rerouted to this FCA, even though there may be a lot of airspace capacity available behind this FCA. Following the same reasoning, in future iterations, the FCA rates will continue being low. In summary, just because the first demand estimation is not accurate, we end up with not fully using a region of airspace and obtain very bad solution.

It can be seen that these two issues are coupled. If there is no demand shift issue, even though a conservative FCA rates policy might not be robust to small demand perturbation, it is in general acceptable, like in the GDP problem. If ideally, FCA rates are optimal with respect to any demand information, then demand shift issue will not be a problem. Even if FCA rates are not ideal, as long as they are not conservative and give flights more reroute opportunities, we may have better FCA rates solution.

In summary, due to TOS-induced demand uncertainty, the dependence on demand information for optimal rates planning, demand shift and conservative FCA rates issues, only suboptimal CTOP FCA rates can be hoped to obtain. In the next section, we will talk about how to develop heuristics to find initial solutions, and how can simulation-based optimization be used to make improvement on these initial search points.

5.4 Simulation-based Optimization, Heuristics

Simulation-based optimization integrates computer simulation with optimization technique. It is often applied to problems in which evaluating a solution involves running simulation models. A classic example is aircraft airfoil design. One has to run complicated computational fluid dynamic models in order to assess a set of proposed parameters [66].

The main reason we consider simulation-based optimization is that it can directly optimize FCA rates without worrying about either conservative FCA rates issue or demand shift issue. However, CTOP rate planning problem is a more challenging problem compared with [50] or [51]. In CTOP, we can have up to 5 FCAs, so the dimension of solution space is much larger than the GDP problem. To provide real-time decision support, a solution needs to be reported in around 5 minutes, which is a more restrictive requirement than in problem [51]. Therefore, tradeoffs and compromises need to be made. In this section, we use simulation-based optimization as a way to do local search and refine the solutions we find using heuristics. Specifically, we adopt the following two-phase approach:

1. In phase one, we use stochastic programming methods and heuristics including saturation technique to quickly find good initial starting points.
2. In phase two, for a subset of FCAs, we employ local search method like pattern search to carefully find better solutions.

Pattern search is classic derivative free local search method. It is composed of two types of moves: *exploratory search*, which is used to find an improving direction by checking points in the neighbourhood; *pattern move*, which searches in the improving direction and will keep move as long as improvement

continues [67]. In CTOP rate planning problem, all decision variables are integers and bounded, therefore small modifications about the original algorithm need to be made to accommodate discrete step size and variable range.

Depending on the complexity of the CTOP use case and the amount of computing power available, more sophisticated heuristics that can potentially find better initial solutions or do more efficient local/global search can be considered. This two-phase pattern search based local search approach is one of many options one can choose from. In this section, we use it to obtain a fully CDM-CTOP compatible solution and compare it with various benchmarks in section 3 and 4.

5.4.1 Three Heuristics

In this section, we introduce three heuristics that are used to find initial search points, and talk about the motivation behind each heuristic.

5.4.1.1 Only Use Capacity Information

In this first heuristic, only capacity information is used to determine FCA rates, which is the approach the FAA will probably prefer to take today. For example, FCA1 is created to limit the traffic flow into PCA1. Then planned acceptance rates of FCA1 are set the same as the reduced capacity of PCA1. The reduced capacity can be obtained from weather translation model (section 2.1.4). In probabilistic weather forecast case, usually the most likely capacity scenario can be used as FCA rates. In this work, the FCA rates are obtained by doing linear interpolation of three capability scenarios. In this way, we can clearly see the trade-off between conservative and nonconservative FCA rates.

5.4.1.2 Saturation Technique, Non-iterative Version

To alleviate the impact of demand shift issue, we want to find approximate upper bounds of FCA acceptance rates, which could allow flights to reroute to previously not fully utilized resources. Through several iterations of computation, we hope a good planned acceptance rates that enable flights to take better use of all resources can be obtained. To get approximate upper bounds of FCA rates, saturation technique introduced in [64] will be used. There are different ways to apply this technique.

In the previous version, we will not use any TOS information, and will simply apply high demand to all FCAs in each time period and solve a single stochastic programming problem.

In this version, no demand information is used and solution is solely dependent on the topology of the FCA-PCA network and the scenario-based capacities of PCAs. And we do not need to run CTOP slot allocation algorithm.

5.4.1.3 Demand Guided Saturation Technique, Iterative Version

In the second version, demand information and rate computation loop are used together with saturation technique in setting FCA rates. The algorithm is as follows:

1. Increase demands to FCAs *proportionally* to sufficiently large numbers .
2. If the demand to a FCA is 0 at a time period, we will set it as some default small value like 1, such that the planned acceptance rate is not always zero.
3. Run CTOP slot allocation algorithm based on the rates obtained, obtain a new demand estimation, go to step 1. Exit if the rates are satisfactory.

5.4.2 Experimental Results

To test the performance of simulation-based optimization, we continue using the test case with convective weather activity in southern Washington Center (ZDC) and EWR airport. We assume there is a four-hour capacity reduction in ZDC/EWR from 2000Z to 2359Z. By analyzing the traffic trajectory and weather data, we can build the FCA-PCA network, shown in Figure 7. In this use case, each

FCA directly lies atop of the corresponding PCA. As we discussed section 5.2.2, ideally there should be two FCAs in front of PCA1, instead of just FCA1. However, the FCA-PCA network in Figure 7 is what most air traffic manager would design and it is what our subject matter experts recommended. In this case, FCA rates will be calculated in directly (section 5.2.4) using the solutions from the static aggregate model.

The CTOP TOS allocation algorithm and stochastic flow simulation algorithm (appendix) are coded in Python. Evaluating one FCA rates policy takes around 0.3 second.



Figure 21: Linear Interpolation of Capacity Scenarios

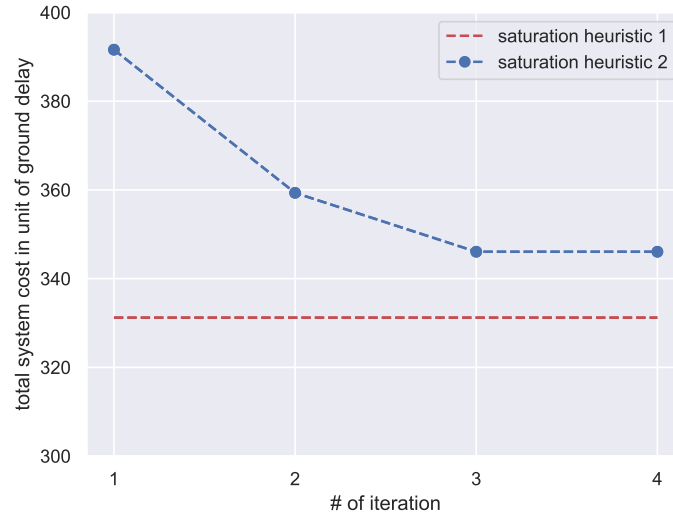


Figure 22: Performance of Saturation Heuristics

5.4.2.1 First Phase Results

Figure 21 shows the result for the capacity interpolation heuristic (the first heuristic). In this use case, the capacity in scenario 1 is strictly better than scenario 2, which is in turn better than scenario 3. In Figure 21, the leftmost bar corresponds scenario 3. A lot of ground delay costs are occurred because of the very conservative FCA rate policy. The rightmost bar corresponds to scenario 1. We see a lot

more air delay because of aggressively large FCA rates. The bars in middle are first phase solutions obtained by the capacity interpolation heuristic.

Figure 22 shows the performance of two saturation heuristics. Second saturation heuristic takes four iterations to converge, which performs slightly worst than first saturation heuristic (346.06 versus 331.19). It happens in this case the FCA rates obtained from first saturation heuristic are the same as from capacity interpolation results, which also happen to be the same as the second capacity scenario (Table 2).

After these initial search points are obtained, in phase 2 pattern search is used to find better FCA rates. To reduce the dimensionality of the search space, only FCA rates of EWR and FCA0 will be further improved in the next phase, because they are the most congested two PCAs (Figure 10 and 11).

5.4.2.2 Second Phase Results

From the starting point obtained in the first saturation heuristic and capacity interpolation, pattern search converges in 3.7 minutes and reduces the system cost from 331.19 to 324.39 (2.1% decrease).

From the starting point obtained in the second saturation heuristic, pattern search converges in 3.7 minutes and reduces the system cost from 346.06 to **324.36** (6.3% decrease). The final solution is listed in Table 10, which is close but not the same as the second capacity scenario.

It can be seen that pattern search method is quite efficient and effective in further reducing the system cost, and multiple starting points can help to find the best final solution.

Table 10: FCA Rates Final Solution

Resource	20:00	15	30	45	21:00	15	30	45	22:00	15	30	45	23:00	15	30	45	00:00	15	30	45	01:00	15	30	45
FCA0	13	14	13	13	13	13	13	13	13	13	24	25	25	25	26	25	25	25	25	25	25	25	25	25
FCA1	44	44	44	44	44	44	44	44	44	44	50	50	50	50	50	50	50	50	50	50	50	50	50	50
FCA2	2	5	5	5	5	5	5	5	5	5	5	5	5	5	5	5	5	5	5	5	5	5	5	5
EWR	8	8	9	9	9	7	8	8	8	8	10	11	10	10	9	11	10	10	10	10	10	10	10	10

5.4.3 Compare with Benchmarks

It is interesting to compare the objective value of simulation-based optimization model with the benchmarks we got in sections 3 and 4, even though they are the objective values of slightly different problems.

In the two-phase simulation-based model, equity is built-in because of the CTOP slot allocation algorithm. In static aggregate model (section 3.4), flights do not have reroute options and the equity issue is not *explicitly* considered (see the discussion in section 3.9). In the two-stage disaggregate model (section 4.2), the goal is to minimize system cost without considering any equity issue.

1. Compared with static aggregate model without reroute whose objective value is 404.0, simulation-based model achieves a lower system cost (324.36). If equity issue is explicitly considered in aggregate model, it is expected that the gap will be even larger. This shows the benefit of allowing rerouting in the face of congestion.
2. Compared with two-stage disaggregate model whose objective value is 167.07, the objective value of simulation-based model is almost two times larger. This shows the price of fairness.

5.5 Conclusions

In this section, we discussed in detail about the properties of FCA-PCA network, and revealed why problem 3 (section 1.3) is substantially more challenging due to TOS-induced demand uncertainty, the dependence on demand information for optimal rates planning, demand shift and conservative FCA rates issues. We proposed a two-phase simulation-based optimization framework which combines stochastic optimization model, saturation heuristic and local search. Through a representative use case, we have demonstrated that this framework is efficient and effective.

6 Contributions

The contributions of this paper are now summarized:

1. We first addressed a simplified CTOP planning problem: assume each flight only has one route option, how to optimally management traffic flow rates to minimize system-wide delay cost? We revealed why it is in nature a multi-commodity flow problem, and gave the correct boundary conditions for such a problem. Three aggregate stochastic programming models are proposed, which can dynamically ground hold flights by exploiting weather and flight schedule information. These aggregate models not only play an integral role in CTOP FCA rates optimization, but can also be used in air traffic flow simulation.
2. Two families of disaggregate stochastic models are then proposed, which generalize the classic GDP planning models to the case of having multiple constrained resources multiple reroute options. In the stochastic optimization framework, the dynamic stochastic models can give the theoretic lower bound for the system delay and reroute costs.
3. We revealed that planned acceptance rates proposed by aggregate CTOP models may be set lower than necessary simply because there was not sufficient demand to warrant a higher rates, and investigated the impact of demand uncertainty on these models.
4. This work gives the first algorithm that optimizes CTOP FCA rates under both demand and capacity uncertainty and is compatible with the CDM-CTOP framework, which provides much-needed decision support capabilities for effective application of CTOP.
5. All nine CTOP related stochastic programming models have good formulation properties and are promising in computation time. They can be coded in decision support tools to help air traffic managers implement and perform post-analysis for air traffic flow programs.

A CTOP Algorithm

A.1 Assumptions

- There is only one activate TMI, which is the CTOP being implemented. TMI interaction is not considered
- Pop-up flights or cancelled flights are not considered
- Trajectory Valid Start Time (TVST), End Time (TVET), and Route Minimum Notification Time (RMNT) restrictions are not considered
- For simplicity, assume the start and end times for all FCAs are the same

A.2 Algorithm Input

- For each FCA r , its activation time, acceptance rate P_t^r at each 15 minutes time period and filters
- For each flight, the unimpeded FCA arrival time for each of its TOS option

A.3 Slot Creation

We create evenly spaced slots for each time period based on given acceptance rate. The i -th slot in time period t FCA r is:

$$\text{slot}_t^r(i) = \text{round}((i - 1) \times \frac{15 \times 60}{P_t^r}) \quad (84)$$

A.3.1 Example 1

The acceptance rate at FCA1 from 00:00Z to 00:15Z is 1. Then slot space is 900s. The slot is at 00:00:00Z.

A.3.2 Example 2

The acceptance rate at FCA1 from 00:00Z to 00:15Z is 3. Then slot space is 300s. The slots are at 00:00:00Z, 00:05:00Z, 00:10:00Z.

A.4 Slot Allocation Algorithm

Algorithm 1 CTOP TOS Allocation Algorithm [68]

- 1: Determine flights included by the CTOP program. A flight is included in CTOP if any TOS route intersect any of the CTOP's FCAs during active periods
 - 2: Determine flights that are part of CTOP demand but are exempted
 - 3: Assign slots to exempted flights first
 - 4: Sort flights by Initial Arrival Time (IAT), which is the earliest FCA arrival time at any of a CTOP's FCAs using any of the flight's TOS options
 - 5: Once at a time, in IAT order, assign each flight the lowest adjusted cost trajectory and slot
-

If a TOS route intersect two or more FCAs. Take the second FCA as an example: slot will be marked as used by finding the first available slot in this FCA that has a time equal or later than the time at the flight would intersect this FCA if flight departing at its ETD, which would include any delay first (primary) FCA imposes.

A.4.1 Example

Flight AA609 has two TOS options. The scheduled departure time is 00:00Z.

- The first TOS option intersects FCA1 with unimpeded arrival time 02:00Z, and land at destination airport with unimpeded arrival time 03:00Z. The RTC for route 1 is 0. If taking route 1, the first available slot at FCA 1 is 02:05Z, the first available slot at destination airport at/after 03:05Z is 03:15Z. The adjusted cost is:

$$\text{RTC} + \text{Assigned ground delay} = 0 + 5 = 5 \text{ minutes}$$

- If second TOS option intersects FCA2 with unimpeded arrival time 02:15Z, and land at destination airport with unimpeded arrival time 03:15Z. The RTC for route 2 is 15. If taking route 2, the first available slot at FCA2 is at 02:15Z, the first available slot at destination airport at/after 03:15Z is 03:15Z. The adjusted cost is:

$$\text{RTC} + \text{Assigned ground delay} = 15 + 0 = 15 \text{ minutes}$$

- Route 1 will be assigned to AA609, even though flight will have to take 5 minutes ground delay and 10 minutes air delay.

A.5 Stochastic Flow Simulation Algorithm

We will only consider the cost for non-exempted flights. The total cost is composed of three parts: reroute cost, ground delay cost incurred by FCAs, air delay cost incurred by PCAs capacity constraints. After we run the CTOP allocation algorithm, we can easily calculate the costs of first two parts, and we will know $S_{t,\rho}^k$, which is the number of flights that will reach PCA k on path ρ in time period t . By solving the following optimization problem, we will know the third part.

$$\min \quad c_a \sum_{q \in \mathcal{Q}} p_q \sum_{t \in \mathcal{T}} \sum_{\rho \in \mathcal{P}} \sum_{k \in \rho} A_{t,\rho}^{k,q} \quad (85)$$

$$L_{t,\rho}^{k,q} = \begin{cases} \text{if } k = \rho_1 & S_{t,\rho}^k - (A_{t,\rho}^{k,q} - A_{t-1,\rho}^{k,q}) \\ \text{else} & \text{UpPCA}_{t,\rho}^{k,q} - (A_{t,\rho}^{k,q} - A_{t-1,\rho}^{k,q}) \end{cases} \quad \forall t \in \mathcal{T}, q \in \mathcal{Q}, \rho \in \mathcal{P}, k \in \rho \quad (86)$$

$$\text{UpPCA}_{t,\rho}^{k,q} = L_{t-\Delta^{k',k},\rho}^{k',q} \quad \forall t \in \mathcal{T}, q \in \mathcal{Q}, (k', k) \in \rho \quad (87)$$

$$\sum_{\rho \in \mathcal{P}} L_{t,\rho}^{k,q} \leq M_{t,q}^k \quad \forall t \in \mathcal{T}, q \in \mathcal{Q}, k \in \mathcal{P} \quad (88)$$

$$L_{t,\rho}^{k,q}, A_{t,\rho}^{k,q} \in \mathbb{Z}_+ \quad \forall t \in \mathcal{T}, q \in \mathcal{Q}, \rho \in \mathcal{P}, k \in \rho \quad (89)$$

References

- [1] Federal Aviation Administration, “Air Traffic By the Numbers,” Tech. rep., 2019.
- [2] Federal Aviation Administration, “FAA Aerospace Forecast Fiscal Years 2019-2039,” Tech. rep., 2019.
- [3] Barnhart, C., Bertsimas, D., Caramanis, C., and Fearing, D., “Equitable and efficient coordination in traffic flow management,” *Transportation science*, Vol. 46, No. 2, 2012, pp. 262–280.
- [4] Rodionova, O., Arneson, H., Evans, A., and Sridhar, B., “Efficient Trajectory Options Allocation for the Collaborative Trajectory Options Program,” 36th Digital Avionics Systems Conference, 2017.
- [5] Smith, N. M., Brasil, C., Lee, P. U., Buckley, N., Gabriel, C., Mohlenbrink, C. P., Omar, F., Parke, B., Speridakos, C., and Yoo, H.-S., “Integrated demand management: Coordinating strategic and tactical flow scheduling operations,” *16th AIAA Aviation Technology, Integration, and Operations Conference*, 2016, p. 4221.
- [6] Odoni, A. R., *The flow management problem in air traffic control*, Springer, 1987, pp. 269–288.
- [7] NBAA, “Ground Delay Program (GDP),” <https://www.nbaa.org/ops/airspace/tfm/tools/gdp.php>, 2019, Accessed: 2019-5-1.
- [8] Abdelghany, A. and Abdelghany, K., *Modeling applications in the airline industry*, Routledge, 2009.
- [9] Hoffman, R. L., *Integer programming models for ground-holding in air traffic flow management*, Ph.D. thesis, University of Maryland at College Park, 1998.
- [10] Barnhart, C., Belobaba, P., and Odoni, A. R., “Applications of operations research in the air transport industry,” *Transportation science*, Vol. 37, No. 4, 2003, pp. 368–391.
- [11] Vossen, T. W., Hoffman, R., and Mukherjee, A., *Air traffic flow management*, Springer, 2012, pp. 385–453.
- [12] Doble, N., Brennan, M., Arora, N., Ermatinger, C., and Clover, S., “Simulation and operational analysis of airspace flow programs for traffic flow management,” *6th AIAA Aviation Technology, Integration and Operations Conference (ATIO)*, 2006, p. 7828.
- [13] Brennan, M., “Airspace flow programs - A fast path to deployment,” *The Journal of Air Traffic Control*, Vol. 49, No. 1, 2007, pp. 51–55.
- [14] NBAA, “Airspace Flow Program (AFP),” <https://nbaa.org/aircraft-operations/airspace/tfm/airspace-flow-program-afp/>, 2019, Accessed: 2019-5-1.
- [15] CSC, “TFMS Functional Description, Appendix C: Traffic Management Initiative (TMI) Algorithms,” Tech. rep., 2014.
- [16] Federal Aviation Administration, “Introduction to Collaborative Trajectory Options Program (CTOP),” https://cdm.fly.faa.gov/?page_id=983, 2018, Accessed: 2018-11-19.
- [17] Steiner, M., Bateman, R., Megenhardt, D., Liu, Y., Xu, M., Pocerich, M., and Krozel, J., “Translation of ensemble weather forecasts into probabilistic air traffic capacity impact,” *Air Traffic Control Quarterly*, Vol. 18, No. 3, 2010, pp. 229–254.
- [18] Clarke, J.-P. B., Solak, S., Ren, L., and Vela, A. E., “Determining stochastic airspace capacity for air traffic flow management,” *Transportation Science*, Vol. 47, No. 4, 2012, pp. 542–559.

- [19] Matthews, M., DeLaura, R., Veillette, M., Venuti, J., and Kuchar, J., “Airspace Flow Rate Forecast Algorithms, Validation, and Implementation,” Project report atc-428, MIT Lincoln Laboratory, Lexington, MA, 2015.
- [20] Liu, P.-c. B., Hansen, M., and Mukherjee, A., “Scenario-based air traffic flow management: From theory to practice,” *Transportation Research Part B: Methodological*, Vol. 42, No. 7, 2008, pp. 685–702.
- [21] Buxi, G. and Hansen, M., “Generating day-of-operation probabilistic capacity scenarios from weather forecasts,” *Transportation Research Part C: Emerging Technologies*, Vol. 33, 2013, pp. 153–166.
- [22] Bertsimas, D. and Patterson, S. S., “The air traffic flow management problem with enroute capacities,” *Operations Research*, Vol. 46, No. 3, 1998, pp. 406–422.
- [23] Bertsimas, D. and Patterson, S. S., “The traffic flow management rerouting problem in air traffic control: A dynamic network flow approach,” *Transportation Science*, Vol. 34, No. 3, 2000, pp. 239–255.
- [24] Bertsimas, D., Lulli, G., and Odoni, A., *The air traffic flow management problem: An integer optimization approach*, Springer, 2008, pp. 34–46.
- [25] Menon, P. K., Sweriduk, G. D., and Bilimoria, K. D., “New approach for modeling, analysis, and control of air traffic flow,” *Journal of Guidance, Control, and Dynamics*, Vol. 27, No. 5, 2004, pp. 737–744.
- [26] Sun, D., Strub, I. S., and Bayen, A. M., “Comparison of the performance of four Eulerian network flow models for strategic air traffic management,” *Networks and Heterogeneous Media*, Vol. 2, No. 4, 2007, pp. 569.
- [27] Sun, D. and Bayen, A. M., “Multicommodity Eulerian-Lagrangian large-capacity cell transmission model for en route traffic,” *Journal of Guidance, Control, and Dynamics*, Vol. 31, No. 3, 2008, pp. 616–628.
- [28] Cao, Y. and Sun, D., “Link transmission model for air traffic flow management,” *Journal of Guidance, Control, and Dynamics*, Vol. 34, No. 5, 2011, pp. 1342–1351.
- [29] Wei, P., Cao, Y., and Sun, D., “Total unimodularity and decomposition method for large-scale air traffic cell transmission model,” *Transportation Research Part B: Methodological*, Vol. 53, 2013, pp. 1–16.
- [30] Birge, J. R. and Louveaux, F., *Introduction to stochastic programming*, Springer Science & Business Media, 2011.
- [31] Richetta, O. and Odoni, A. R., “Solving optimally the static ground-holding policy problem in air traffic control,” *Transportation Science*, Vol. 27, No. 3, 1993, pp. 228–238.
- [32] Richetta, O. and Odoni, A. R., “Dynamic solution to the ground-holding problem in air traffic control,” *Transportation Research Part A: Policy and Practice*, Vol. 28, No. 3, 1994, pp. 167–185.
- [33] Ball, M. O., Hoffman, R., Odoni, A. R., and Rifkin, R., “A stochastic integer program with dual network structure and its application to the ground-holding problem,” *Operations Research*, Vol. 51, No. 1, 2003, pp. 167–171.
- [34] Kotnyek, B. and Richetta, O., “Equitable models for the stochastic ground-holding problem under collaborative decision making,” *Transportation Science*, Vol. 40, No. 2, 2006, pp. 133–146.

- [35] Mukherjee, A. and Hansen, M., “A dynamic stochastic model for the single airport ground holding problem,” *Transportation Science*, Vol. 41, No. 4, 2007, pp. 444–456.
- [36] Ben-Tal, A., El Ghaoui, L., and Nemirovski, A., *Robust optimization*, Vol. 28, Princeton University Press, 2009.
- [37] Gupta, S., *A tractable optimization framework for Air Traffic Flow Management addressing fairness, collaboration and stochasticity*, Ph.D. thesis, Massachusetts Institute of Technology, 2012.
- [38] Sroková, M., *The Air Traffic Flow Management Problem under Capacity Uncertainty: A Robust Optimization Approach*, Master’s thesis, Università degli Studi dell’Aquila, 2015.
- [39] Bertsimas, D., Brown, D. B., and Caramanis, C., “Theory and applications of robust optimization,” *SIAM review*, Vol. 53, No. 3, 2011, pp. 464–501.
- [40] Clare, G. and Richards, A., “Air traffic flow management under uncertainty: application of chance constraints,” Proceedings of the 2nd international conference on application and theory of automation in command and control systems, 20–26, IRIT Press, 2012.
- [41] Chen, J. and Sun, D., “Stochastic Ground-Delay-Program Planning in a Metroplex,” *Journal of Guidance, Control, and Dynamics*, Vol. 41, No. 1, 2017, pp. 231–239.
- [42] Jones, J. C., DeLaura, R., Pawlak, M., Troxel, S., and Underhill, N., “Predicting & Quantifying Risk in Airport Capacity Profile Selection for Air Traffic Management,” *12th USA/Europe Air Traffic Management Research and Development Seminar, Seattle, USA*, 2017.
- [43] Liu, P.-c. B. and Hansen, M., “Scenario-free sequential decision model for the single airport ground holding problem,” *7th USA/Europe Air Traffic Management Research and Development Seminar, Barcelona, Spain*, 2007.
- [44] Cox, J. and Kochenderfer, M. J., “Probabilistic airport acceptance rate prediction,” *AIAA Modeling and Simulation Technologies Conference*, 2016, p. 0165.
- [45] Cox, J. and Kochenderfer, M. J., “Ground Delay Program Planning Using Markov Decision Processes,” *Journal of Aerospace Information Systems*, 2016, pp. 134–142.
- [46] Grabbe, S. R., Sridhar, B., and Mukherjee, A., “Similar days in the NAS: an airport perspective,” *2013 Aviation Technology, Integration, and Operations Conference*, 2013, p. 4222.
- [47] Kuhn, K. D., “A methodology for identifying similar days in air traffic flow management initiative planning,” *Transportation Research Part C: Emerging Technologies*, Vol. 69, 2016, pp. 1–15.
- [48] Estes, A. and Lovell, D., “Identifying Representative Traffic Management Initiatives,” *International Conference on Research in Air Transportation*, 2016.
- [49] Bloem, M. and Bambos, N., “Stochastic models of Ground Delay Program implementation for prediction, simulation, and insight,” *Journal of Aerospace Operations*, Vol. 5, No. 1-2, 2017, pp. 85–117.
- [50] Cook, L. S. and Wood, B., “A model for determining ground delay program parameters using a probabilistic forecast of stratus clearing,” *Air Traffic Control Quarterly*, Vol. 18, No. 1, 2010, pp. 85–108.
- [51] Taylor, C., Masek, T., and Wanke, C., “Designing Traffic Flow Management Strategies Using Multiobjective Genetic Algorithms,” *Journal of Guidance, Control, and Dynamics*, Vol. 38, No. 10, 2015, pp. 1922–1934.

- [52] Mukherjee, A. and Hansen, M., “A dynamic rerouting model for air traffic flow management,” *Transportation Research Part B: Methodological*, Vol. 43, No. 1, 2009, pp. 159–171.
- [53] Liu, Y. and Hansen, M., “Evaluation of the performance of ground delay programs,” *Transportation Research Record*, Vol. 2400, No. 1, 2014, pp. 54–64.
- [54] Liu, Y. and Hansen, M., “Incorporating predictability into cost optimization for ground delay programs,” *Transportation Science*, Vol. 50, No. 1, 2015, pp. 132–149.
- [55] Conforti, M., Cornuéjols, G., and Zambelli, G., *Integer programming*, Vol. 271, Springer, 2014.
- [56] Walter, M. and Truemper, K., “Implementation of a Unimodularity Test,” *Mathematical Programming Computation*, Vol. 5, No. 1, 2013, pp. 57–73.
- [57] Evans, J. R. and Jarvis, J. J., “Network topology and integral multicommodity flow problems,” *Networks*, Vol. 8, No. 2, 1978, pp. 107–119.
- [58] Zhu, G., Wei, P., Hoffman, R., and Hackney, B., “Centralized Disaggregate Stochastic Allocation Models for Collaborative Trajectory Options Program (CTOP),” 37th AIAA/IEEE Digital Avionics Systems Conference (DASC), London, 2018.
- [59] Zhu, G., Wei, P., Hoffman, R., and Hackney, B., “Aggregate Multi-commodity Stochastic Models for Collaborative Trajectory Options Program (CTOP),” International Conference on Research in Air Transportation (ICRAT), Barcelona, Spain, 2018.
- [60] Zhu, G. and Wei, P., “An Interval-based TOS Allocation Model for Collaborative Trajectory Options Program,” 2018, AIAA Aviation, Atlanta, GA.
- [61] Bertsimas, D., Farias, V. F., and Trichakis, N., “The price of fairness,” *Operations research*, Vol. 59, No. 1, 2011, pp. 17–31.
- [62] Bertsimas, D. and Gupta, S., “Fairness and collaboration in network air traffic flow management: an optimization approach,” *Transportation Science*, Vol. 50, No. 1, 2015, pp. 57–76.
- [63] Mukherjee, A., Hansen, M., and Grabbe, S., “Ground delay program planning under uncertainty in airport capacity,” *Transportation Planning and Technology*, Vol. 35, No. 6, 2012, pp. 611–628.
- [64] Zhu, G., Wei, P., Hoffman, R., and Hackney, B., “Saturation Technique for Optimizing Planned Acceptance Rates in Traffic Management Initiatives,” The 21st IEEE International Conference on Intelligent Transportation Systems, Hawaii, 2018.
- [65] Hoffman, R., Hackney, B., Zhu, G., and Wei, P., “Enhanced Stochastic Optimization Model (ESOM) for Setting Flow Rates in a Collaborative Trajectory Options Program (CTOP),” AIAA Aviation, Atlanta, GA, 6 2018.
- [66] Koziel, S., Leifsson, L., and Yang, X.-S., *Simulation-Driven Modeling and Optimization*, Springer, 2016.
- [67] Chinneck, J. W., *Practical optimization: a gentle introduction*, Carleton University, Ottawa. <http://www.sce.carleton.ca/faculty/chinneck/po.html>, 2006.
- [68] Kim, B. and Clarke, J.-P., “Optimal Airline Actions during Collaborative Trajectory Options Programs,” AGIFORS 54th Annual Symposium, Dubai, UAE, 2014.